TECHNICAL REPORT HL-89-16

US Army Corps of Engineers

RED RIVER WATERWAY
JOHN H. OVERTON LOCK AND DAM

Report 5
SEDIMENTATION IN LOCK APPROACHES
TABS-2 Numerical Model Investigation

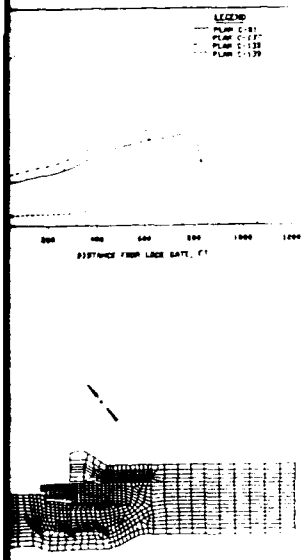

by

Bradley M. Comes, Ronald R. Copeland, William A. Thomas

Hydraulics Laboratory

DEPARTMENT OF THE ARMY
Waterways Experiment Station, Corps of Engineers
3909 Halls Ferry Road
Vicksburg, Mississippi 39180-6199

August 1989
Report 5 of a Series

HYDRAULICS LABORATORY

Prepared for US Army Engineer District, Vicksburg
Vicksburg, Mississippi 39181-0060

SECURITY CLASSIFICATION OF THIS PAGE

REPORT DOCUMENTATION PAGE

Form Approved OMB No. 0704-0188

1a. REPORT SECURITY CLASSIFICATION: Unclassified	1b. RESTRICTIVE MARKINGS
2a. SECURITY CLASSIFICATION AUTHORITY	3. DISTRIBUTION / AVAILABILITY OF REPORT: Approved for public release; distribution unlimited.
2b. DECLASSIFICATION / DOWNGRADING SCHEDULE	
4. PERFORMING ORGANIZATION REPORT NUMBER(S): Technical Report HL-89-16	5. MONITORING ORGANIZATION REPORT NUMBER(S)
6a. NAME OF PERFORMING ORGANIZATION: USAEWES Hydraulics Laboratory; 6b. OFFICE SYMBOL (If applicable): CEWES-HR-M	7a. NAME OF MONITORING ORGANIZATION
6c. ADDRESS (City, State, and ZIP Code): PO Box 631 Vicksburg, MS 39181-0631	7b. ADDRESS (City, State, and ZIP Code)
8a. NAME OF FUNDING / SPONSORING ORGANIZATION: USAED, Vicksburg; 8b. OFFICE SYMBOL (If applicable)	9. PROCUREMENT INSTRUMENT IDENTIFICATION NUMBER
8c. ADDRESS (City, State, and ZIP Code): PO Box 60 Vicksburg, MS 39181-0060	10. SOURCE OF FUNDING NUMBERS: PROGRAM ELEMENT NO. / PROJECT NO. / TASK NO. / WORK UNIT ACCESSION NO.

11. TITLE (Include Security Classification)
Red River Waterway, John H. Overton Lock and Dam, Sedimentation in Lock Approaches; TABS-2 Numerical Model Investigation

12. PERSONAL AUTHOR(S)
Comes, Bradley M.; Copeland, Ronald R.; Thomas, William A.

13a. TYPE OF REPORT	13b. TIME COVERED	14. DATE OF REPORT (Year, Month, Day)	15. PAGE COUNT
Report 5 of a series	FROM _____ TO _____	August 1989	59

16. SUPPLEMENTARY NOTATION
Available from National Technical Information Service, 5285 Port Royal Road, Springfield, VA 22161.

17. COSATI CODES		
FIELD	GROUP	SUB-GROUP

18. SUBJECT TERMS (Continue on reverse if necessary and identify by block number)
Navigation lock and dams; Sedimentation; Numerical models; TABS-2 computer program; Red River, Louisiana

19. ABSTRACT (Continue on reverse if necessary and identify by block number)

A two-dimensional numerical model, TABS-2, was used to predict fine sediment deposition in the lock approach channels upstream and downstream from the John H. Overton Lock and Dam on the Red River Waterway, Louisiana. The numerical model was used to evaluate the effects of various design changes on fine sediment deposition. These included changing the length and height of divider dikes, the number of openings on the ported guard wall, the invert elevation in the lock approach channel, and the location of spur dikes.

20. DISTRIBUTION / AVAILABILITY OF ABSTRACT: ☒ UNCLASSIFIED/UNLIMITED ☐ SAME AS RPT ☐ DTIC USERS	21. ABSTRACT SECURITY CLASSIFICATION: Unclassified
22a. NAME OF RESPONSIBLE INDIVIDUAL	22b. TELEPHONE (Include Area Code) / 22c. OFFICE SYMBOL

DD Form 1473, JUN 86 — Previous editions are obsolete. — SECURITY CLASSIFICATION OF THIS PAGE

PREFACE

The numerical model investigation of the Red River upstream and downstream from John H. Overton Lock and Dam, reported herein, was conducted at the US Army Engineer Waterways Experiment Station (WES) at the request of the US Army Engineer District, Vicksburg (LMK). In addition to this numerical model study, three physical model studies of John H. Overton Lock and Dam were conducted at WES: a fixed-bed navigation study (Report 2); a movable-bed sedimentation study (Report 3); and a hydraulic structures model study (Report 4). This is Report 5 of the series. Report 1, to be published later, will summarize all of the physical and numerical modeling studies.

The investigation was conducted during the period December 1985 to January 1987 by personnel of the Hydraulics Laboratory at WES under the direction of Mr. F. A. Herrmann, Jr., Chief of the Hydraulics Laboratory, and Mr. M. B. Boyd, Chief of the Waterways Division. Mr. W. A. Thomas of the Waterways Division provided general guidance and review. The Project Engineers and authors of this report were Mr. R. R. Copeland and Mr. B. M. Comes, Math Modeling Group (MMG). Technical assistance was provided by Ms. Brenda L. Martin, MMG. This report was edited by Mrs. Marsha C. Gay, Information Technology Laboratory, WES.

During the course of this study, close working contact was maintained with Mr. Rick Robertson of the Engineering Division, LMK, who served as the coordinating engineer for LMK, providing required data and technical assistance. During this investigation, many representatives from both engineering staffs attended several meetings at WES and LMK to discuss progress of this investigation and others related to the Red River Waterway.

Acting Commander and Director of WES during preparation of this report was LTC Jack R. Stephens, EN. Technical Director was Dr. Robert W. Whalin.

CONTENTS

CONVERSION FACTORS, NON-SI TO SI (METRIC)
UNITS OF MEASUREMENT

Non-SI units of measurement used in this report can be converted to SI (metric) units as follows:

Multiply	By	To Obtain
cubic feet	0.02831685	cubic metres
cubic yards	0.7645549	cubic metres
feet	0.3048	metres
inches	2.54	centimetres
miles (US statute)	1.609347	kilometres
pounds (force)-second per square foot	47.88026	pascals-second

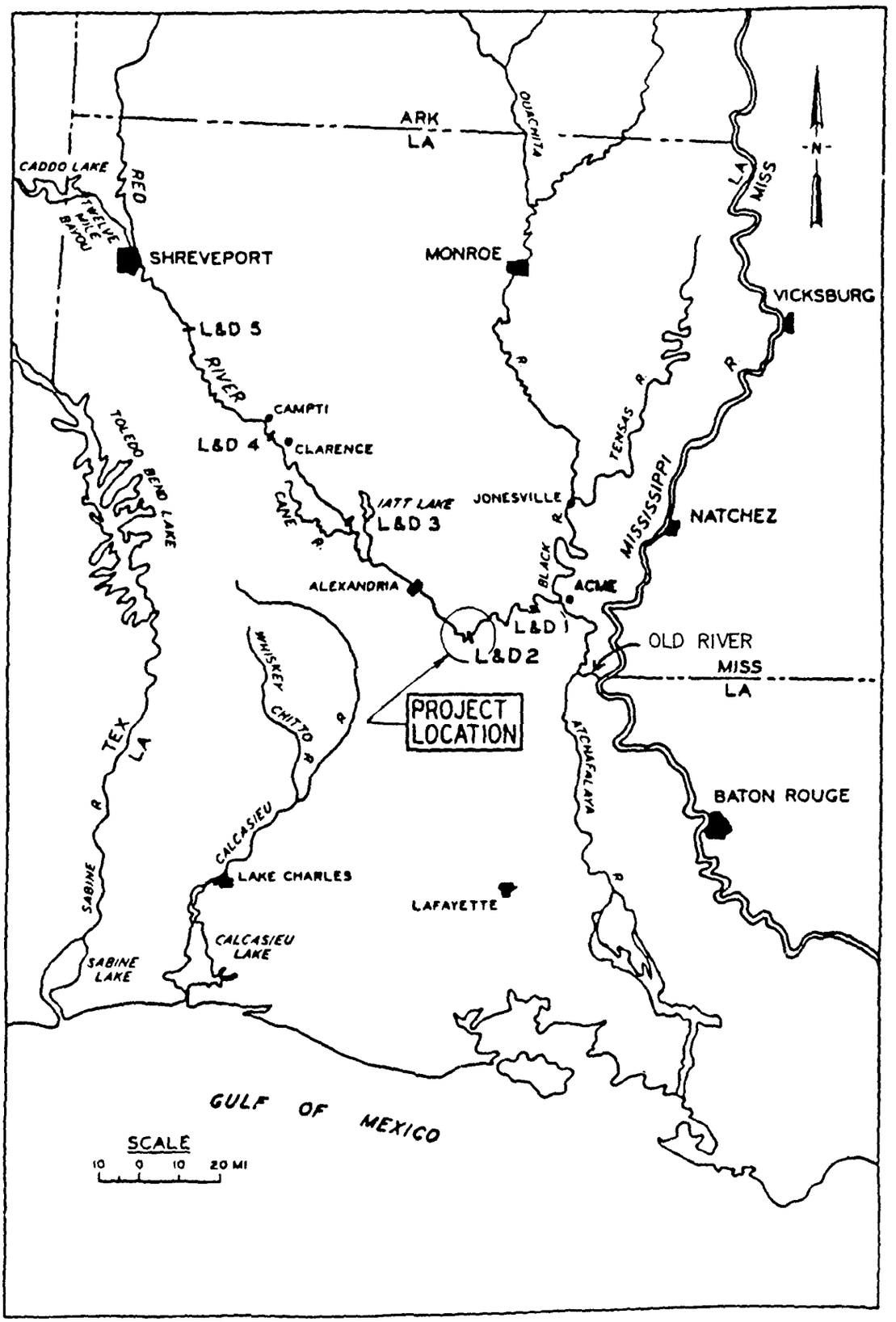

Figure 1. Location map

RED RIVER WATERWAY,
JOHN H. OVERTON LOCK AND DAM
SEDIMENTATION IN LOCK APPROACHES
TABS-2 Numerical Model Investigation

PART I: INTRODUCTION

The Prototype

1. The Red River Waterway Project will provide a navigation route from the Mississippi River at its junction with Old River via the Old and Red rivers to Shreveport, LA. The project will provide a channel 236 miles* long, 9 ft deep, and 200 ft wide and will include a system of five locks and dams to control water levels. The existing river will be realigned as necessary to develop an efficient channel, and bank stabilization and training works will be constructed to hold the newly developed channel in position.

2. John H. Overton Lock and Dam (Lock and Dam No. 2) is located in a river cutoff at 1967 river mile 87.4, which is about 44 river miles upstream from Lock and Dam No. 1 (Figure 1). It consists of a single lock on the left descending side of the cutoff, a 348-ft-long dam with five 60-ft-wide gates, and a 250-ft-long overflow weir with crest at el 66.0** on the right descending side (Figure 2). The lock chamber has a usable length of 685 ft and is 84 ft wide with upstream and downstream miter gate sill elevations of 40.5 and 25.0 ft, respectively. The lock chamber floor is at el 23.0.

3. The river channel upstream from the lock and dam is about 600 ft wide and has a design invert el of 34.0. Three nonovertopping spur dikes are located on the right descending bank just upstream of the cutoff. These dikes were included in the design based on physical model studies (Report 2, Wooley, in preparation) at the US Army Engineer Waterways Experiment Station (WES). The upstream lock approach channel is separated from the spillway entrance channel by a 700-ft-long ported guard wall. The intake manifolds for the

---

* A table of factors for converting non-SI units of measurement to SI (metric) units is presented on page 3.

** All elevations (el) and stages cited herein are in feet referred to the National Geodetic Vertical Datum (NGVD).

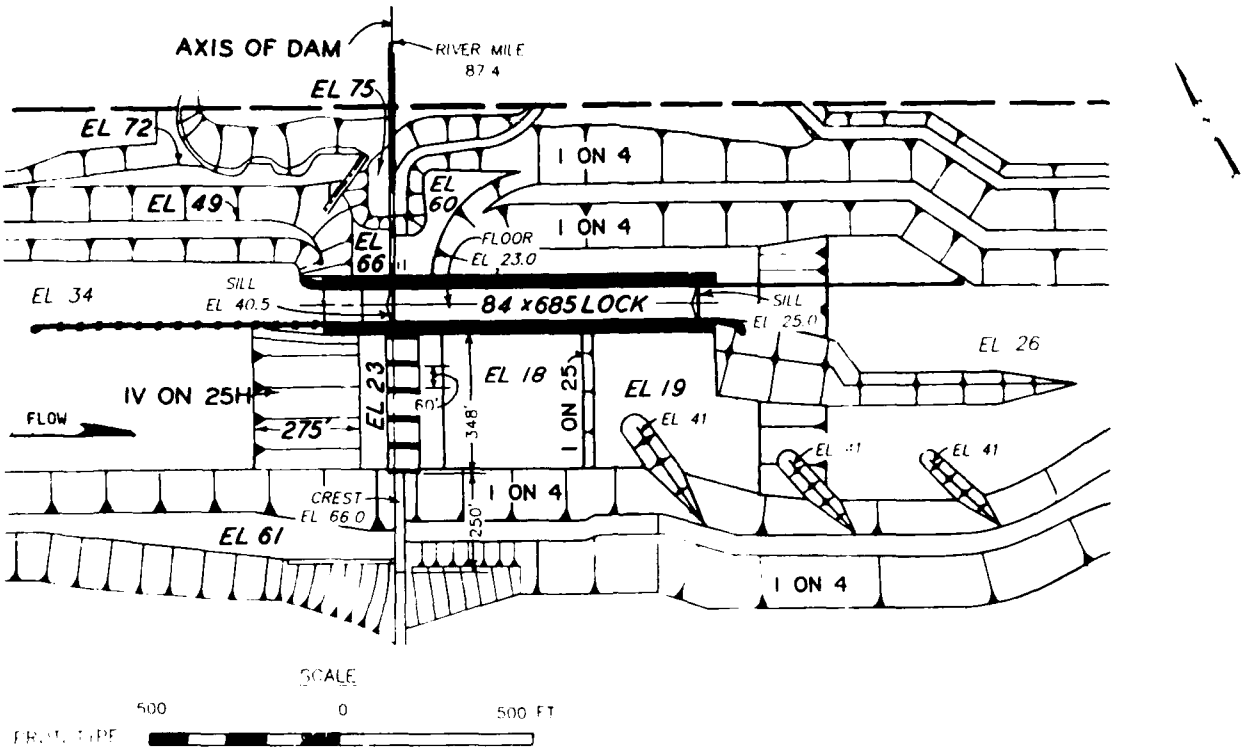

Figure 2. Plan of John H. Overton Lock and Dam

filling system are located in a 170-ft-long lock approach section between the downstream end of the guard wall and the miter gates.

4. The downstream channel is about 250 ft wide and has a design invert el of 26.0. The invert elevation decreases to el 19.0 at the miter gates. A 290-ft-long dike with a crest el of 74.5 separates the downstream lock approach channel from the spillway exit channel. This separation is extended by a 430-ft-long dike with a crest el of 50.0. This latter dike is designed to overtop during high flows, allowing water and suspended sediment into the lock approach channel while retaining sediment bed load in the spillway exit channel. In movable-bed physical model studies conducted at WES (Report 3, O'Neal, in preparation), this design reduced shoaling at the junction of the lock approach and spillway exit channels. Three dikes with crests sloping from el 48.0, land end, to el 41.0, river end, are located in the spillway exit channel on the right descending bank. These dikes facilitate the movement of bed load and were designed using the movable-bed physical model. The dam is designed to maintain a normal pool el of 64.0 and to pass all flows up to the levee design flood. The minimum downstream tailwater is el 40.0, which is the normal pool elevation maintained at Lock and Dam No. 1.

Purpose and Scope of the Model Study

5. Lock and Dam No. 1 on the Red River was opened in the fall of 1984. Deposition of fine sediment in the upstream and downstream lock approach channels was much greater than anticipated. Dredging was required at the entrance to the upstream approach channel and throughout the downstream approach channel. Sediment deposition at the downstream miter gate was severe enough to prevent operations. The lock chamber eventually had to be dewatered and the deposited sediment cleaned out. Two-dimensional numerical model studies were employed by the US Army Engineer District (USAED), Vicksburg, and WES to address the fine sediment problem at Lock and Dam No. 1 (Little 1985, Copeland and Thomas 1988). As a result of these studies, design modifications were recommended and constructed at Lock and Dam No. 1. After 2 years of operations these modifications appear to have significantly reduced the fine sediment problems in the lock approach channels. The same two-dimensional numerical approach was employed at Lock and Dam No. 2 to identify potential sedimentation problems at that site.

6. Separate numerical models were developed for the upstream and downstream approaches to the dam. The downstream model simulated the river for about 0.7 mile from the dam, and the upstream model extended about 2 miles from the dam. These models were used to evaluate fine sediment deposition in the lock approach channels and near the miter gates. The effects of changing the length and height of the dividing dikes were tested in the downstream model. The effects of the ported guard wall, the invert elevation in the lock approach channel, and upstream spur dikes were tested in the upstream model. Results of the numerical modeling of fine sediment deposition were coordinated with physical model studies conducted at WES to achieve a recommended design that adequately satisfied the needs of navigation, bed-load sediment transport, and considerations related to the hydraulic structure itself. The results of the fixed-bed navigation alignment study are given in Report 2 (Wooley, in preparation); the results of the distorted movable-bed model study, in Report 3 (O'Neal, in preparation); and the results of the 1:50-scale structures model, in Report 4 (Maynord and Markussen, in preparation).

PART II: THE MODEL

Description

7. The two-dimensional numerical model study was conducted using the TABS-2 modeling system (Thomas and McAnally 1985). This system provides two-dimensional solutions to open-channel and sediment problems using finite element techniques. It consists of more than 40 computer programs to perform modeling and related tasks. A two-dimensional depth-averaged hydrodynamic numerical model, RMA-2V, was used to generate the current patterns. The current patterns were then coupled with the sediment properties of the river and used as input to a two-dimensional sedimentation model, STUDH. The other programs in the system perform digitizing, mesh generation, data management, graphical display, output analysis, and model interfacing tasks. Although TABS-2 may be used to model unsteady flow, only steady-state conditions were simulated in this study. Hydrographs were simulated by a series of steady-state events. Input data requirements for the hydrodynamic model, RMA-2V, include channel geometry, Manning's roughness coefficients, turbulent exchange coefficients, and boundary flow conditions. The sediment model, STUDH, requires hydraulic parameters from RMA-2V, sediment characteristics, inflow concentrations, and sediment diffusion coefficients. Sediment is represented by a single grain size, and transport potential is calculated using the Ackers-White equation (Ackers and White 1973). Due to the uncertainty related to the turbulent exchange and diffusion coefficients in the two models, prototype and/or physical model data for adjustment purposes are highly desirable.

Finite Element Network

8. Finite element networks were developed to simulate about 0.7 mile of the Red River downstream from Lock and Dam No. 2 (Figure 3) and 2.0 miles upstream (Figure 4). The downstream network contained 927 elements and included lock approach and spillway exit channels, dikes, and the navigation exit channel. The upstream network contained 2,104 elements and included the lock and spillway approach channels, 1.5 miles of natural river upstream of the cutoff, deflector dikes, the overflow weir, and the ported guard wall. Conveyance through the ported guard wall was simulated in a depth-averaged sense

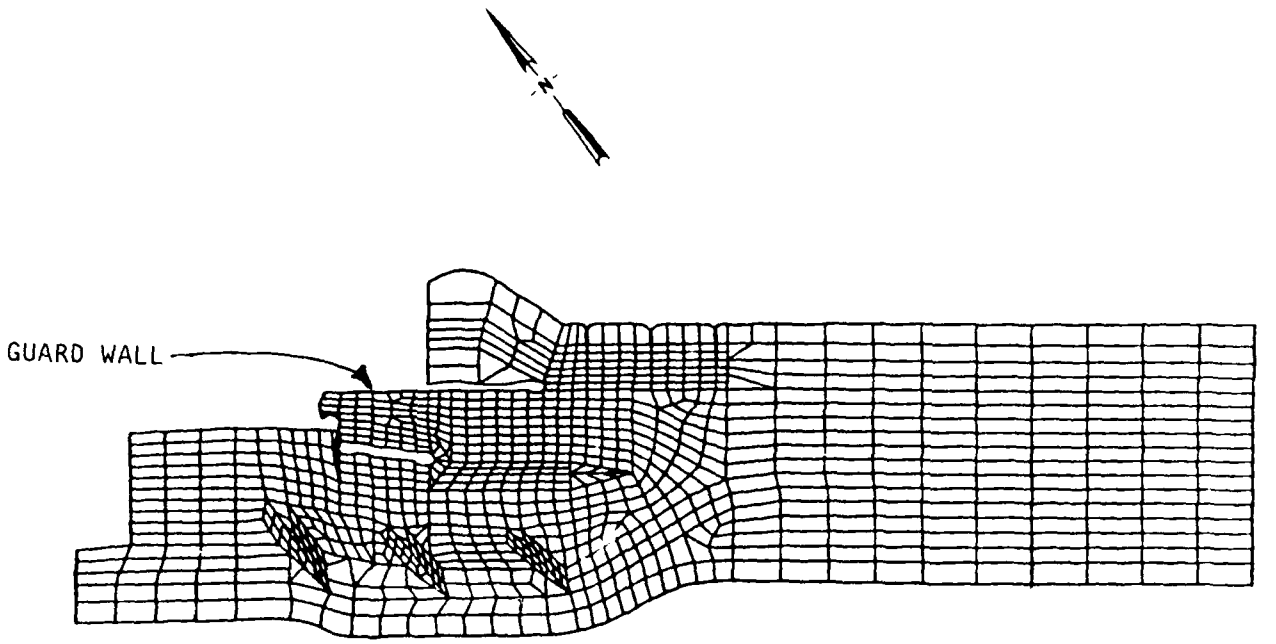

Figure 3. Finite element network downstream from the lock and dam

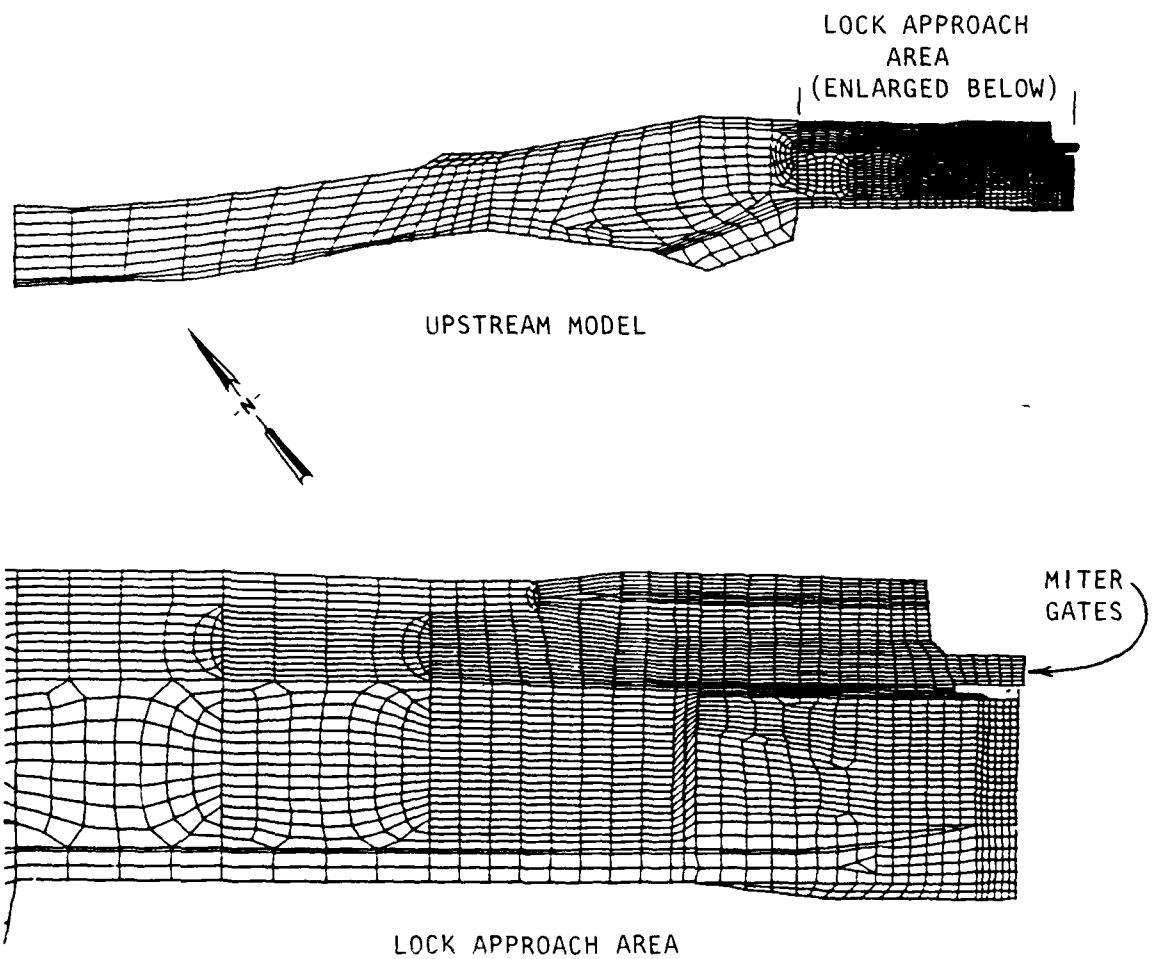

Figure 4. Finite element network upstream of the lock and dam

by treating the wall as a weir, adjusting the crest elevation to achieve the correct flow area, and increasing Manning's roughness coefficients to account for pier losses. Grid resolution behind the guard wall was increased to allow the model to reproduce eddies. Initial bed elevations for both models were obtained from construction drawings and represent conditions prior to opening of the structure. Slip boundaries were specified for most of the grid perimeter, allowing velocities to be calculated at these locations and eliminating the need for fine grid resolution adjacent to the boundary where the lateral velocity gradient is steep. Some of the boundary nodes were specified as "stagnation points," i.e., locations of zero velocity. These specifications are generally located in corners of the grid or along boundaries with negligible flow velocities and are employed to ease calculation of slopes for slip boundaries. Tailwater was assigned at the downstream boundary of each grid and inflow distribution specified at the upstream boundary. Grid boundary specifications are shown in Figures 5 and 6.

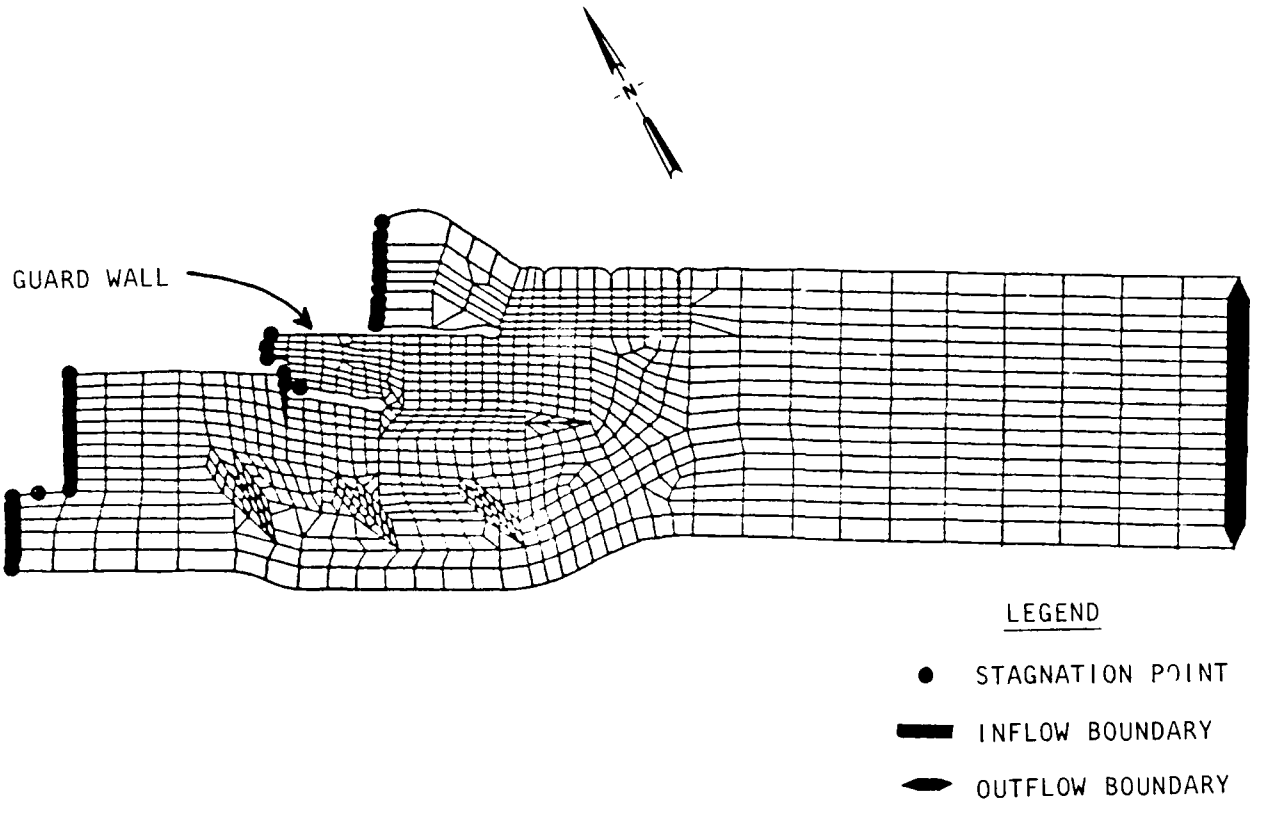

Figure 5. Network boundary conditions downstream of lock and dam

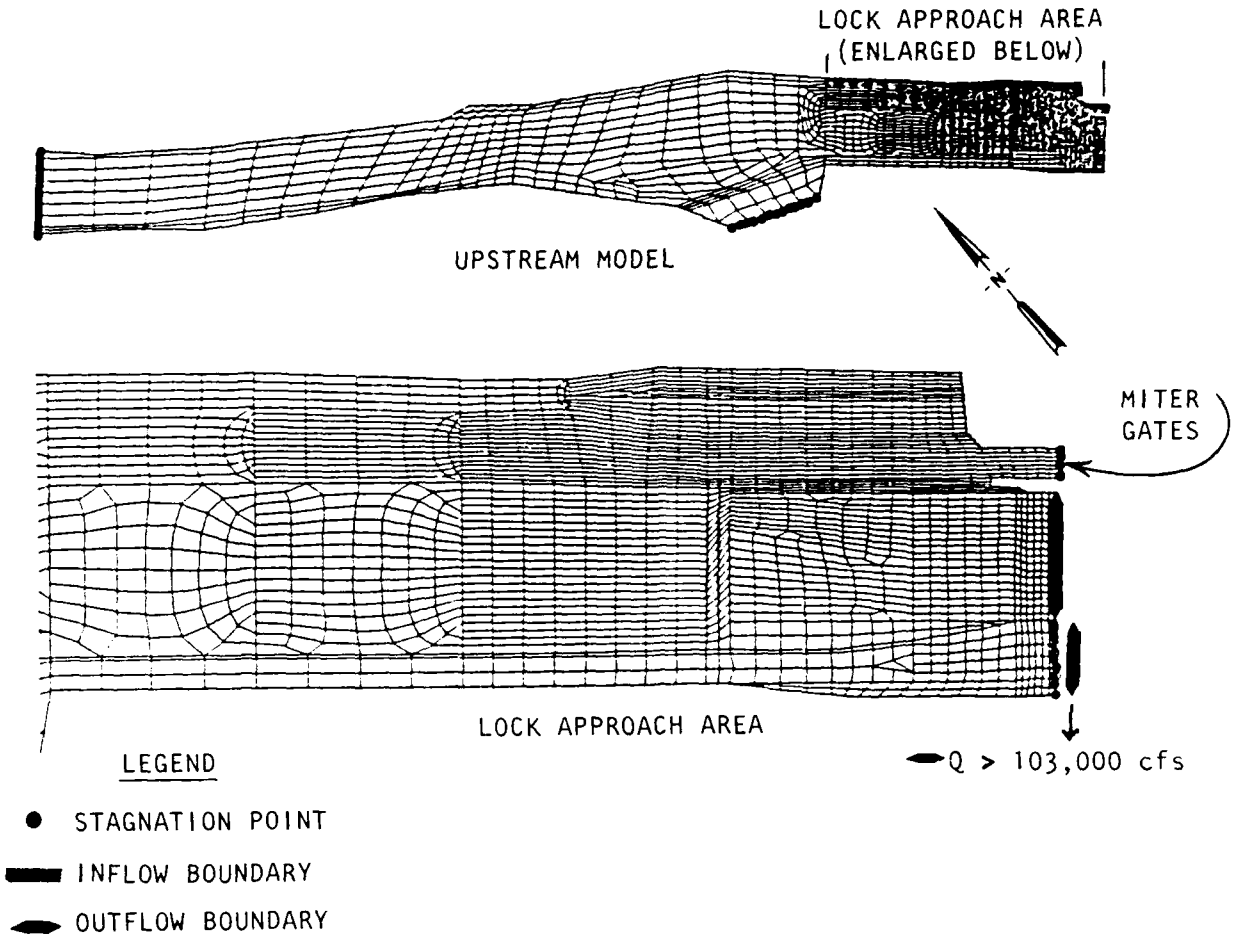

Figure 6. Network boundary conditions upstream of lock and dam

Hydrodynamic Boundary Conditions

9. Spillway gates carry the total flow up to a discharge of about 103,000 cfs. At greater discharges, the flow is divided between the spillway gates and the overflow weir. Flow distributions through these structures were calculated by the Vicksburg District (Figure 7).

10. For the downstream model, the inflow distribution across the overflow weir was assumed to be uniform. Distribution through the spillway gates was based on measurements from the structures physical model since distributions from the upstream numerical model were not available when this portion of the study was conducted. Measurements were taken at each gate bay on the structures physical model for discharges of 80,000 and 120,000 cfs. Distribution percentages were similar for both discharges. Looking downstream with

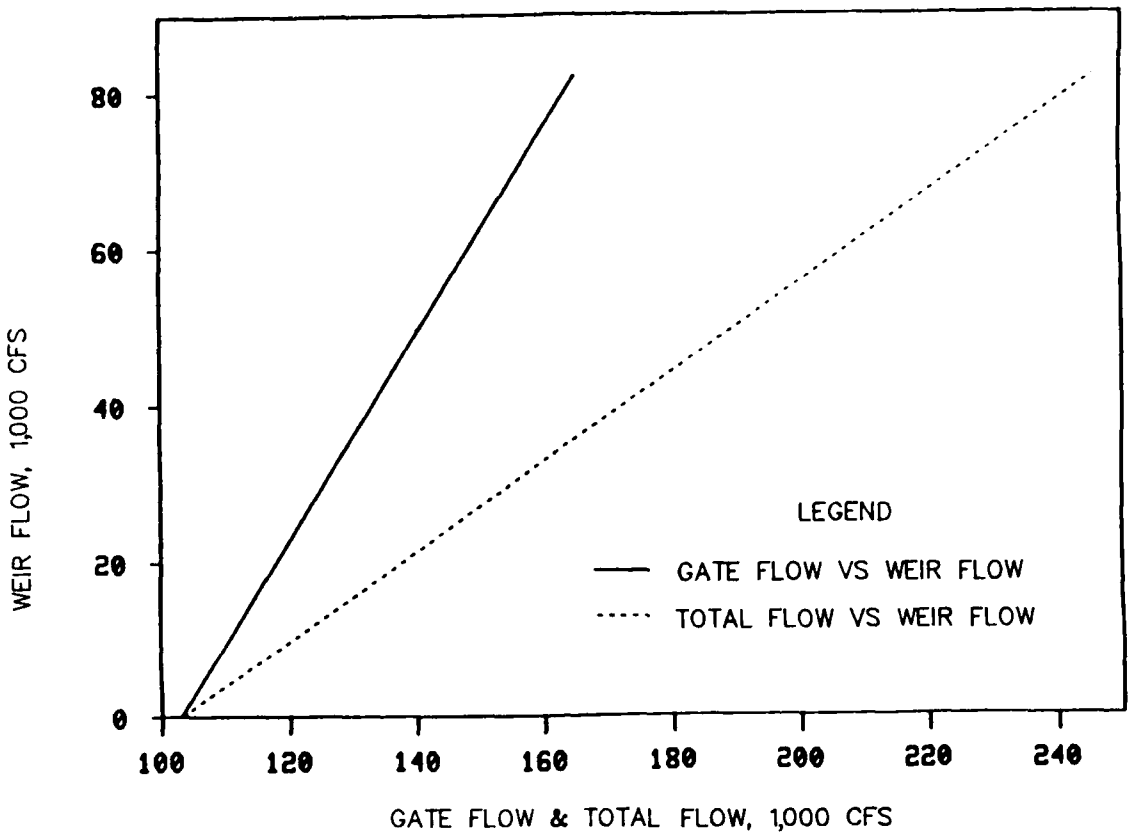

Figure 7. Flow distribution through gates and weir

gate bay No. 1 on the left, adopted flow percentages through bays 1, 2, 3, 4, and 5 were 13, 17, 27, 22, and 21, respectively. A later check found that the upstream numerical model produced flow percentages of 13, 21, 22, 24, and 20, respectively. The adopted flow percentages were used to calculate unit discharges that were used as input into RMA-2V.

11. For the upstream model, the discharge distribution was specified to produce a uniform velocity distribution across the upstream model boundary. The lateral velocity distribution became fully developed as the flow passed the three dikes on the right descending bank.

12. Tailwater elevations for both numerical models were based on the published tailwater rating curve at Lock and Dam No. 2 (USAED, New Orleans, 1980b). The tailwater boundary for the downstream model was located 0.7 mile from the dam. Water-surface elevation slopes (USAED, New Orleans, 1980a) were used to calculate the tailwater at the downstream model boundary. This calculation produced a water-surface elevation at the dam that was 0.5 ft lower than the published tailwater for discharges greater than 30,000 cfs. Normal pool elevation upstream of the dam is 64 ft. This water-surface elevation was

held for discharges up to 95,000 cfs. Head losses through the structure for large discharges were determined by Vicksburg District and added to the published tailwater rating curve to determine the tailwater rating curve for the upstream model. Tailwater rating curves used in the numerical models are shown in Figure 8.

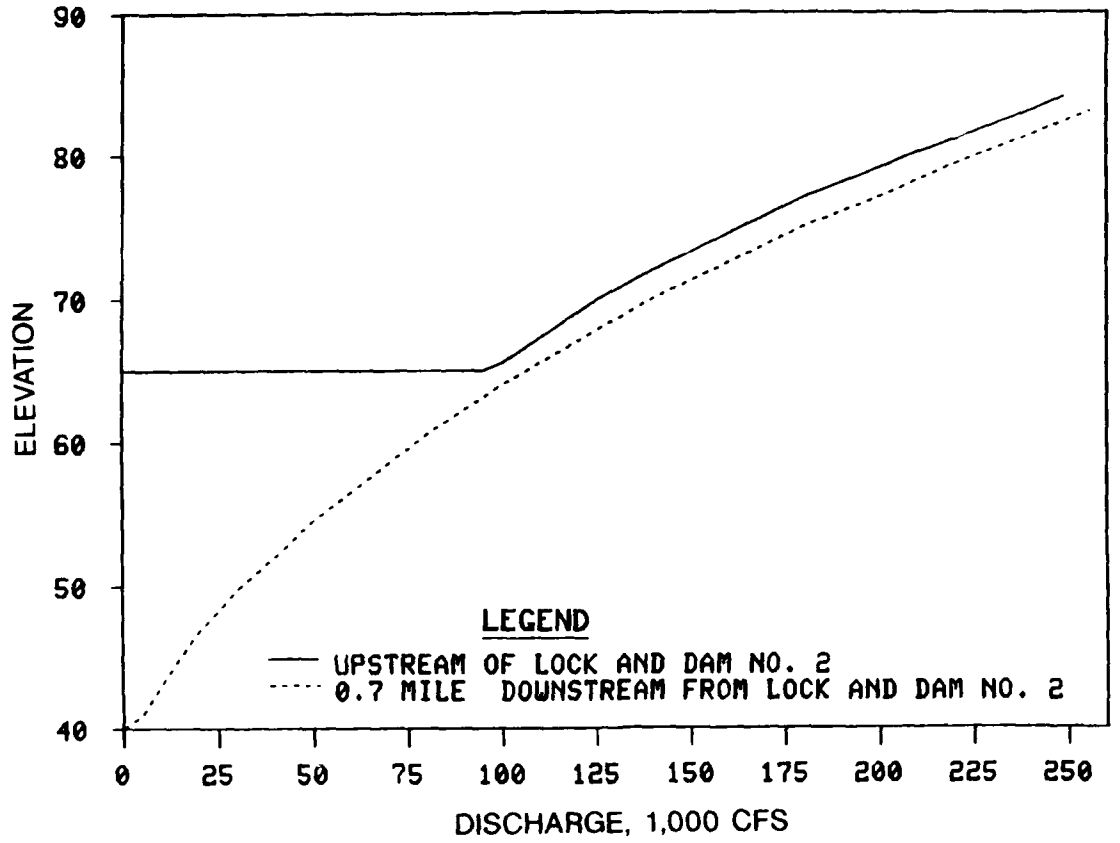

Figure 8. Tailwater and headwater rating curves

Roughness Coefficients

13. Manning's roughness coefficients were assigned to each element using measured data and the Limerinos equation (Limerinos 1970), which includes relative roughness as a variable. The roughness coefficient for elements on the channel bottom with a sand bed was set at 0.017. This value, used by Vicksburg District in their study upstream of Lock and Dam No. 1 (Little 1985), is based on grain size and water-surface elevation adjustments to their numerical model. Riprap placed on the channel bottom and side slopes and on dikes had a median particle size D_{50} that varied between 10 and 36 in. The Limerinos equation

$$n = \frac{0.0926R^{0.1667}}{1.16 + 2.0 \log (R/D_{84})} \quad (1)$$

where

n = Manning's roughness coefficient

R = hydraulic radius

D_{84} = particle size of which 84 percent of the bed is finer

was used to calculate roughness coefficients for the different features through a range of depth. Average depths were used to calculate a roughness coefficient on side slopes. Calculated values were adjusted slightly to account for additional losses based on comparisons to measured data from the 1:50-scale structures physical model. The following roughness coefficients were assigned in the numerical model:

Feature	Assigned Value
Sand bottom	0.017
Riprap bottom	0.040
Riprap side slope <el 50	0.045
Riprap side slope >el 50	0.055
Main longitudinal dike (downstream)	0.050
Riprap berm	0.045
Upstream guard wall (submerged weir)	0.060
Submerged dikes (downstream, right descending bank)	0.060
Dike field (downstream, left descending bank)	0.060

These values are compatible with those used in previous work at Lock and Dam No. 1. The three dikes on the upstream right descending bank were modeled as zero-width slip boundaries; i.e., two slip boundaries on top of each other, one for the upstream side of the dike and the other for the downstream side. Additional roughness is not required for dikes modeled in this manner.

14. Velocity measurements from the 1:50-scale physical model were compared to calculated velocities from the downstream numerical model. Considering the accuracy of both models, calculated and measured results compared favorably. The water-surface profiles for 2,500 ft of the spillway exit channel were essentially identical (Figure 9). Comparisons of calculated and measured velocities indicated that more flow was passing over the longitudinal submerged dike in the numerical model, making measured velocities from the

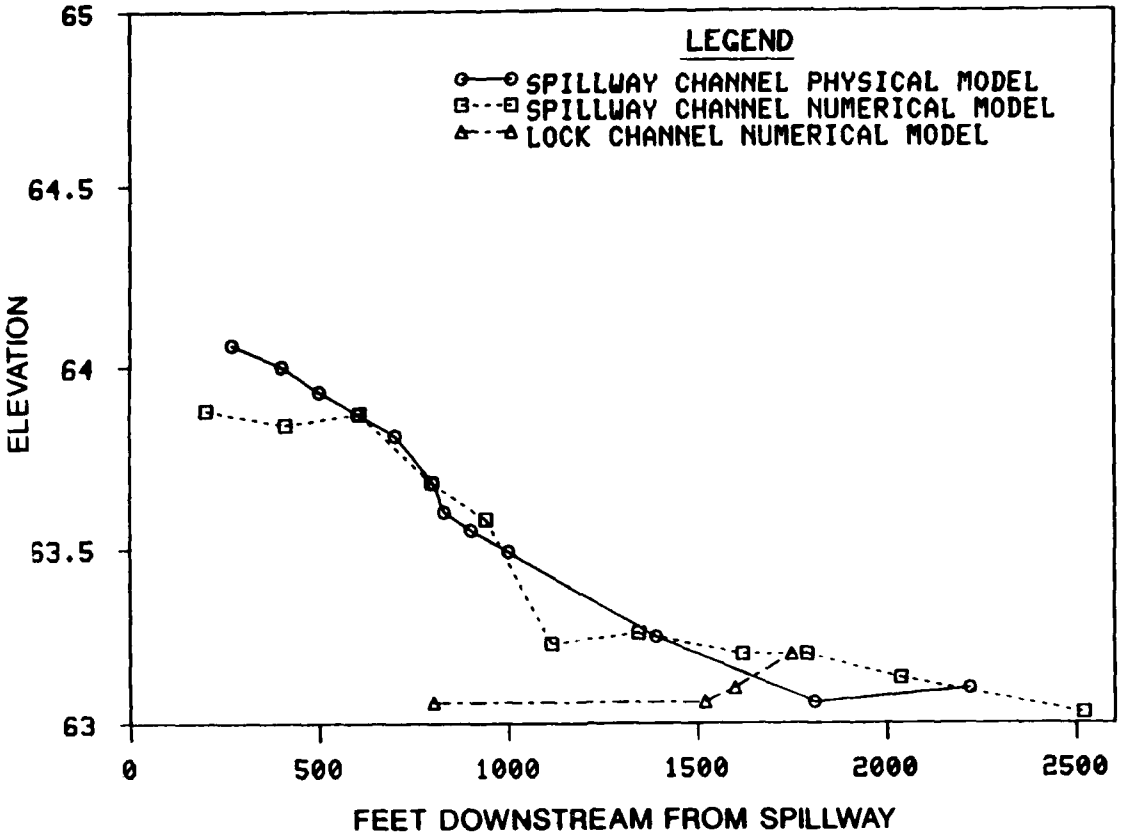

Figure 9. Comparison of physical and numerical water-surface profiles

physical model higher in the spillway exit channel upstream of its confluence with the lock approach channel.

15. The effect of increasing the roughness coefficient for the submerged dikes was tested. An increase in effective roughness may be required to account for increased turbulence due to disturbance of the hydrostatic velocity distribution. A very high value of 0.20 affected the lateral velocity distribution, but did not produce a distribution closer to the velocities measured in the physical model. As shown in Table 1 (measurement locations are shown in Plate 1), velocities in the spillway exit channel increased, becoming closer to measured values, but velocities in the vicinity of the submerged dikes decreased, diverging from measured values. A final test was made using a roughness coefficient of 0.06 for the submerged dikes to account for some increased effective roughness due to turbulence, and roughness coefficients on the overbanks were increased slightly to increase flow in the channel.

16. Manning's n values for the upstream pool of Lock and Dam No. 2

could not be directly adjusted using prototype water-surface profiles. However, results from physical and one-dimensional numerical models were available. A short reach was modeled upstream of the dam in the undistorted 1:50-scale physical model, and long reach lengths were used in the HEC-2 model run by the New Orleans District. Under pool conditions, the slope of the water surface for the length of the model is very small, and small differences in roughness coefficients do not significantly affect the water-surface elevations or the hydrodynamic and sedimentation results. However, under open river conditions, roughness and slope become more critical. The average water-surface slope under these conditions in the numerical model was calculated to be 0.50 ft per mile. This corresponds well with the average slope of 0.45 ft per mile obtained by the New Orleans District (USAED, New Orleans, 1980b).

17. The effect of roughness coefficients on lateral velocity distribution was tested using depth-averaged velocity measurements from the distorted (1:120H, 1:80V) movable-bed physical model. Comparision of normalized lateral velocity profiles at two sections is shown in Figure 10. Considering measurement difficulties in the distorted physical model, the distributions matched very well except for the leftmost point of section 2. With the lateral velocity profiles showing good correspondence with the physical model data, the main channel and side slope Manning's n values were not changed.

18. Roughness coefficient values from 0.017 to 0.060 were tested for the ported guard wall, which was simulated as a submerged weir. With a roughness coefficient of 0.060, the discharge distribution along the wall in the numerical model matched discharge measurements taken from the 1:50-scale physical model. Figure 11 compares the discharge distribution of the physical model's ported guard wall and the numerical model's weir using this adjusted roughness coefficient.

Turbulent Exchange Coefficients

19. Momentum exchanges due to velocity gradients are approximated in RMA-2V by multiplying a turbulent exchange coefficient times the second derivative of the velocity with respect to the x- and y-directions. Limited guidance is available for selection of these coefficients. In these studies, calculated eddies and velocity patterns were verified with prototype and

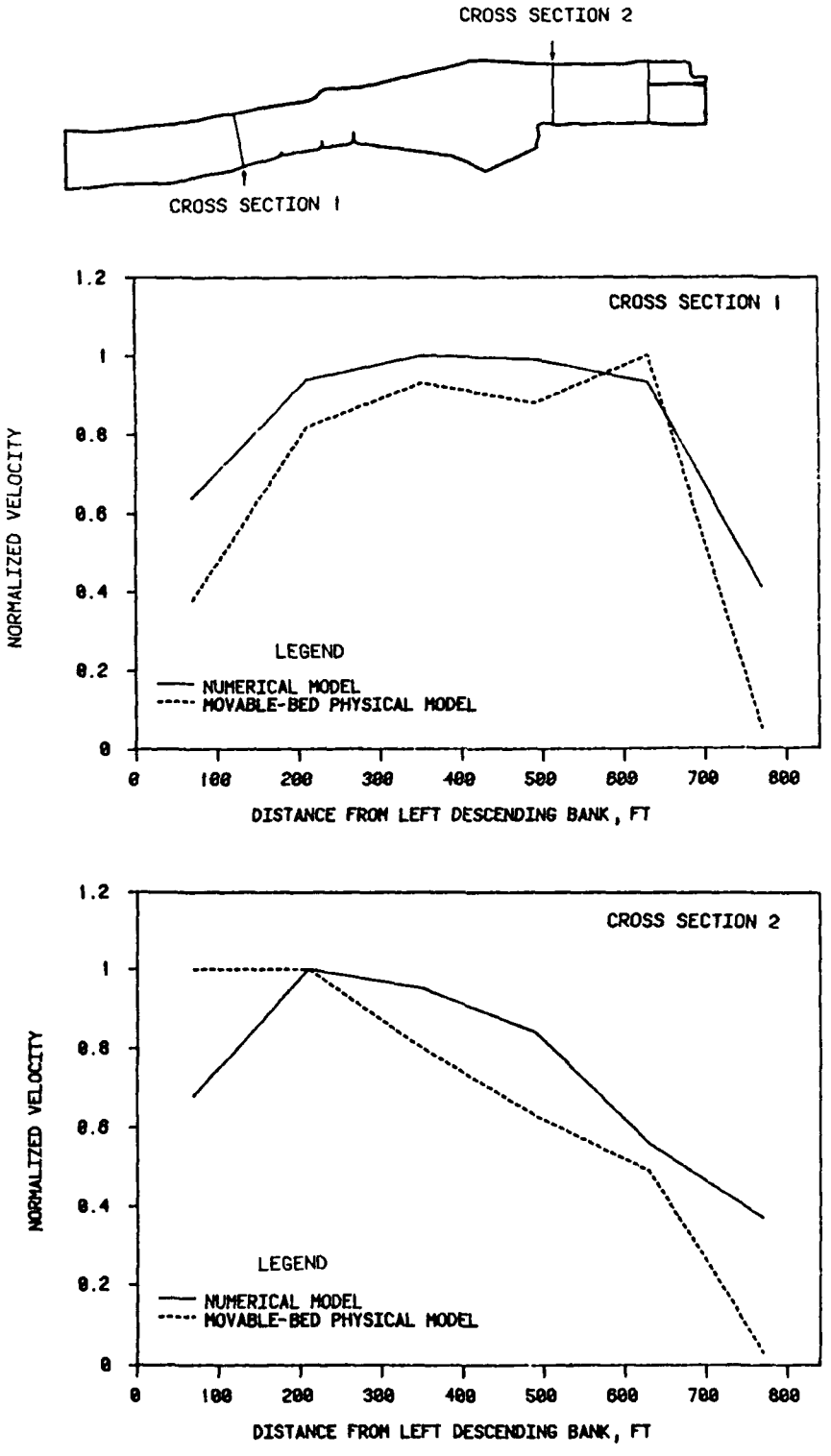

Figure 10. Normalized lateral velocity profiles

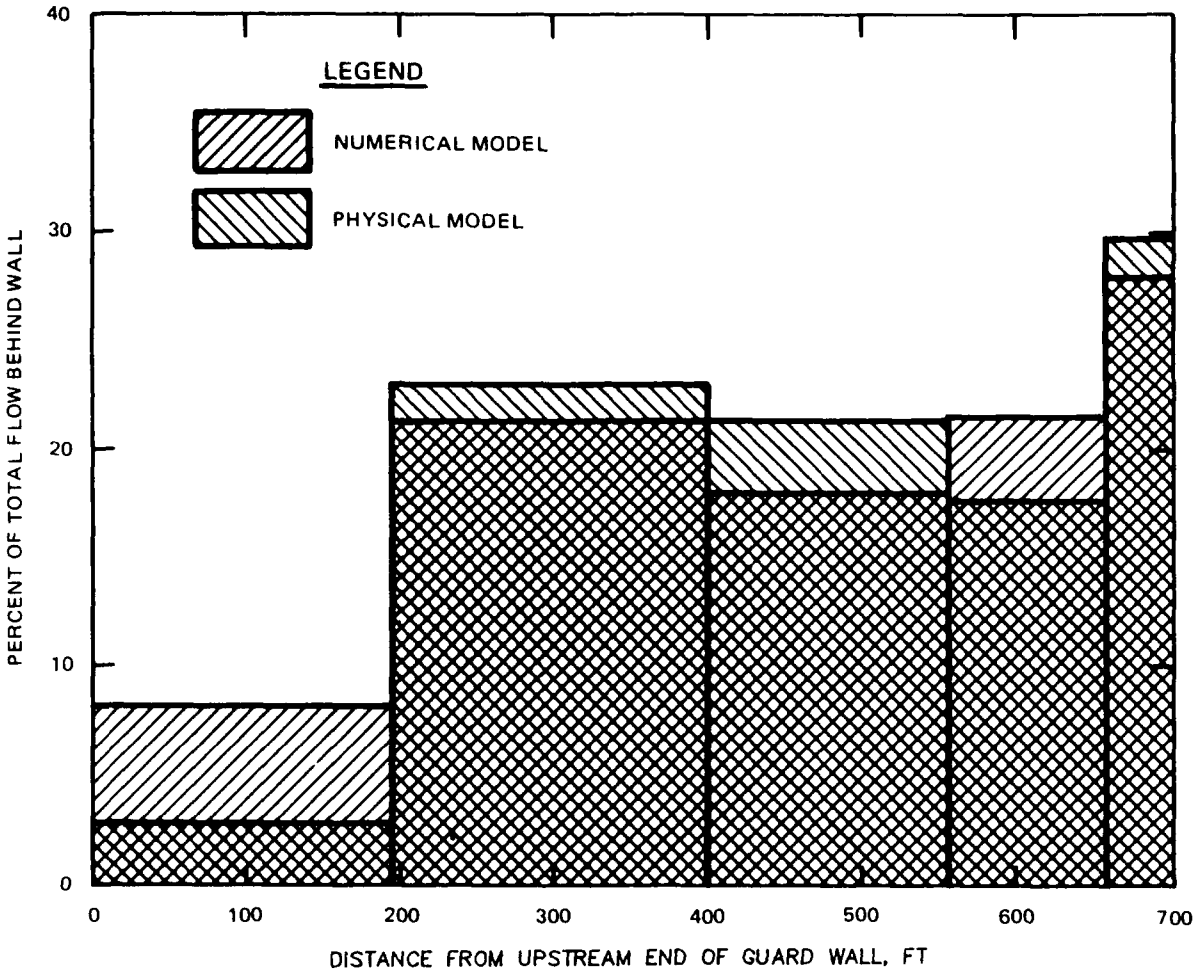

Figure 11. Distribution of flow through guard wall ports

physical model data when the turbulent exchange coefficients varied between 5 and 50 lb-sec/sq ft. Previous sensitivity studies indicated that coefficients of 25 lb-sec/sq ft were satisfactory. For this study, the element size and aspect ratios remained approximately the same and turbulent exchange coefficients of 25 lb-sec/sq ft were selected as initial values subject to additional sensitivity analysis.

20. The effect of the turbulent exchange coefficients on lateral velocity distribution in the numerical model was tested. Velocities were calculated for turbulent exchange coefficients of 5, 10, 12, 25, 50, and 500 lb-sec/sq ft. Results at locations shown in Plate 2 are tabulated in Table 2. Calculated results were compared to measurements from the 1:50-scale physical model (Maynord and Markussen, in preparation). Three sets of measurements are tabulated in Table 2. The variations demonstrate a typical accuracy range for this type of measurement. The Principal Investigator

conducting the physical model study considered the third set of measurements in Table 2 the most accurate, and they were used for comparison. The results indicated that the turbulent exchange coefficients did not significantly affect the lateral velocity distribution. Therefore it was deemed unnecessary to change from the initial values of 25 lb-sec/sq ft.

21. The effect of increasing the turbulent exchange coefficients for the elements describing the three submerged deflection dikes and the submerged longitudinal dike was tested. Raising the value of these coefficients is sometimes required in areas of high turbulence. Coefficients of 200 and 500 lb-sec/sq ft were assigned to the submerged dikes. Because the results, shown in Table 1, indicated no significant change, the coefficients were returned to their initial value.

22. With the adjusted roughness coefficients and a constant turbulent exchange coefficient of 25 lb-sec/sq ft, calculated and measured velocities were compared (Plate 2). Approximately 40 percent of the flow passed over the longitudinal submerged dike into the lock approach channel in the numerical model. In the physical model, 35 percent of the flow passed over the dike, according to calculations using average measured velocities. Differences between the physical and numerical models are considered to be within an acceptable range considering the accuracies of both.

23. Initial turbulent exchange coefficients of 25 lb-sec/sq ft were also used in the upstream model. The coefficients were not adjusted beyond this initial assignment due to the extensive turbulent exchange coefficient adjustments conducted for the downstream reach as well as for other TABS-2 hydrodynamic studies on the Red River. Adjusting the coefficients had little effect on performance of the ported guard wall.

Bed Material

24. The TABS-2 system analyzes sediment movement using a representative grain size. This technique works well with fairly uniform bed material. Unfortunately, bed material size varies considerably around a structure as well as laterally across a channel. For this study, measured data from Lock and Dam No. 1 were applied at Lock and Dam No. 2. This translocation of bed material data was required because Lock and Dam No. 2 was not in operation and direct data were not available. Previous one-dimensional numerical model work

(Copeland and Thomas 1988) demonstrated the reasonableness of this translocation by showing that the variation in average bed material gradation in the Red River downstream from Shreveport is very slight. A short distance upstream from Lock and Dam No. 1, at 1967 river mile 51.5, the median bed material size varied between 0.13 mm at the point bar and 0.65 mm at the thalweg during measurements taken in April and May 1985. Bed samples from deposits in the upstream and downstream lock approach channels at Lock and Dam No. 1 had median diameters between 0.07 and 0.04 mm. Inside the lock chamber itself, a sample near the upstream gate had a median size of 0.028 mm and a sample near the downstream gate had a median size of 0.055 mm. In addition, bed material size was observed to vary with depth in the deposit. This variation with depth is due to layering of different sizes of fairly uniform material and is attributed to changes in flow patterns at different discharges and stages. Since the complex variation of bed material size cannot be accounted for in the numerical model, a representative size must be selected for the area of primary interest.

25. Based on samples taken from the deposit in the Lock and Dam No. 1 upstream lock approach channel in November 1984, the Vicksburg District chose an average grain size of 0.07 mm for their upstream numerical model study (Little 1985). Differences between this measurement and subsequent measurements upstream and downstream from Lock and Dam No. 1 were deemed insufficient to forsake consistency, and an average grain size of 0.07 mm was adopted for numerical simulations of deposition in the lock approach channels at Lock and Dam No. 2.

Sediment Concentration

26. The sediment inflow concentration for the numerical model is a function of the representative grain size used in the study. Only the portion of the total sediment load that contributes to bed changes in the primary area of interest should be included. Using the bed material gradation in the upstream lock approach channel at Lock and Dam No. 1 with a median diameter of 0.07 mm, it was determined that material greater than 0.03 mm would be considered in determining sediment inflow.

27. Suspended sediment data with size class analyses in the silt range, 0.062-0.004 mm, are required to determine the appropriate sediment inflow

concentration. The Vicksburg District obtained suspended sediment measurements upstream from Lock and Dam No. 1 at river mile 51.5 in April and May 1985. At a discharge of 59,500 cfs, a total suspended sediment concentration of 0.771 kg/cu m was measured, and at 93,000 cfs the measured concentration was 1.525 kg/cu m. These concentrations are compared to concentrations at Alexandria, LA, for the period 1971, 1972, and 1975-1981 in Figure 12. The 1985 measured concentrations are within the range of data, but well below average values. This distribution may have occurred because the 1985 data were taken well into the runoff season when concentrations typically decline. The 1985 data did have size class analyses in the silt range so that appropriate sediment concentrations could be determined. Fifty-three percent of the total measured suspended load was greater than 0.03 mm. This was the percentage used to develop the sediment inflow rating curves.

28. Extrapolation and interpolation of the two 1985 data points were used to determine sediment inflow for qualitative studies with 10-day durations at discharges of 90,000 and 145,000 cfs. A regression curve of the

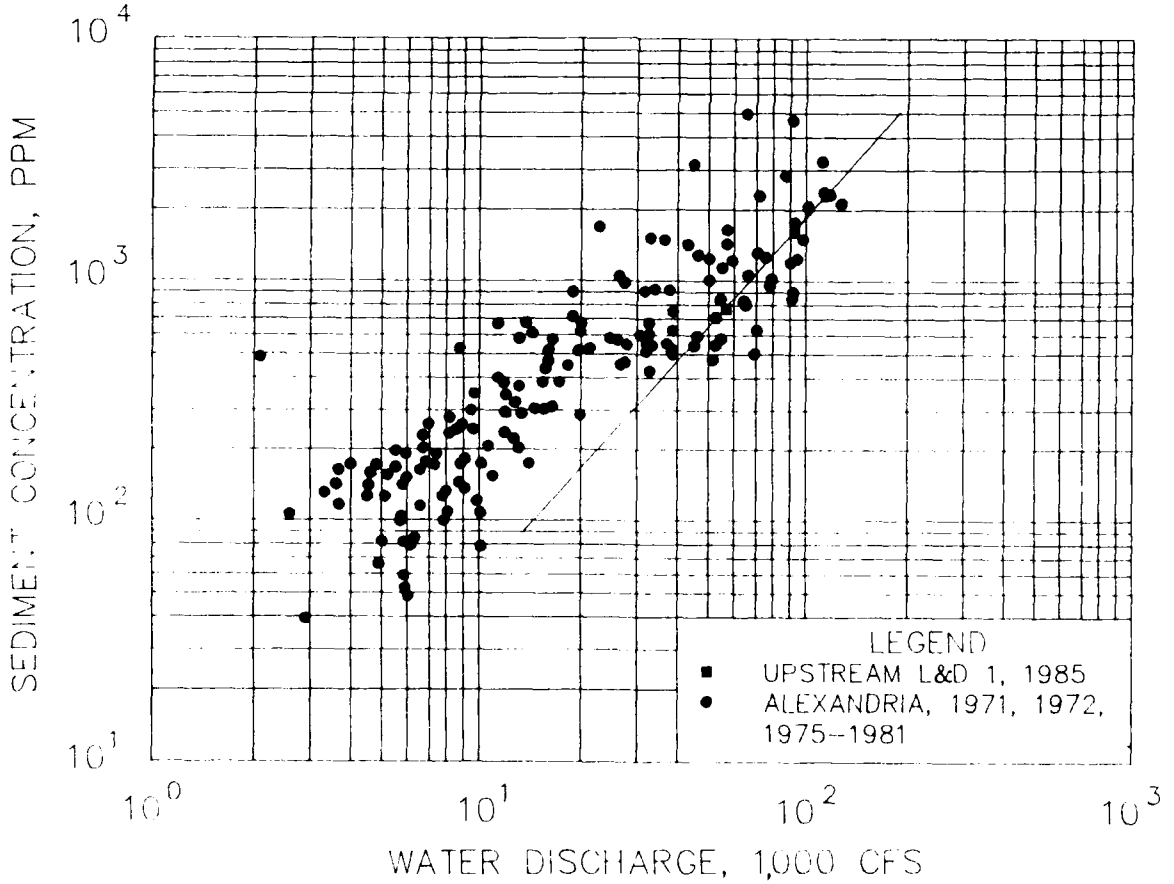

Figure 12. Inflowing sediment concentrations

total measured suspended load at Alexandria, LA, was multiplied by 0.53 to obtain a sediment inflow rating curve for the typical hydrograph in the downstream numerical model. The typical hydrograph (Plate 3) is the 1972 annual hydrograph, which was chosen by the Vicksburg District to represent an average runoff year. Using this sediment concentration curve at low flow rates in the upstream model caused significant deposition at the upstream end of the model. This deposition was attributed to decreased sediment transport capacity due to the pool. The influence of the pool extended upstream beyond the limit of the numerical model, making it necessary to revise the sediment inflow rating curve. An iterative process was used to determine sediment concentration capacity in the numerical model for several flows. At discharges of 75,000 cfs and greater, fine sediment deposition in the main channel was insignificant as most of the inflowing load was transported through the system. At discharges lower than 75,000 cfs, the difference between the reduced regression curve and the transport capacity under pool conditions was determined to represent the volume of material deposited for the 10 months preceding the typical hydrograph peak. This volume was used to increase the concentration of the peak flow. Using this procedure, the inflowing concentrations were adjusted for hydraulic conditions while the average annual sediment yield was maintained. Adopted sediment inflow rating curves used for the upstream reach are shown in Figure 13. The resuspended concentration, at 135,000 cfs, is the concentration that was calculated for the peak flow.

Sediment Diffusion Coefficients

29. The same sediment diffusion coefficients used in the numerical model studies of Lock and Dam No. 1 (Copeland and Thomas 1988) were used in these studies. Sensitivity studies conducted as part of those studies indicated that calculated deposition was not sensitive to the sediment diffusion coefficient in areas where flow is moving generally in a downstream direction and conveyance is the primary driving force affecting sediment movement. However, in essentially dead-water areas, such as in front of the lock miter gates, where deposition is primarily a function of diffusion, the sediment diffusion coefficients are critical. Reproduction of hydrographic survey data from the upstream and downstream lock approach channels at Lock and Dam No. 1 was used to determine the appropriate coefficients for these models.

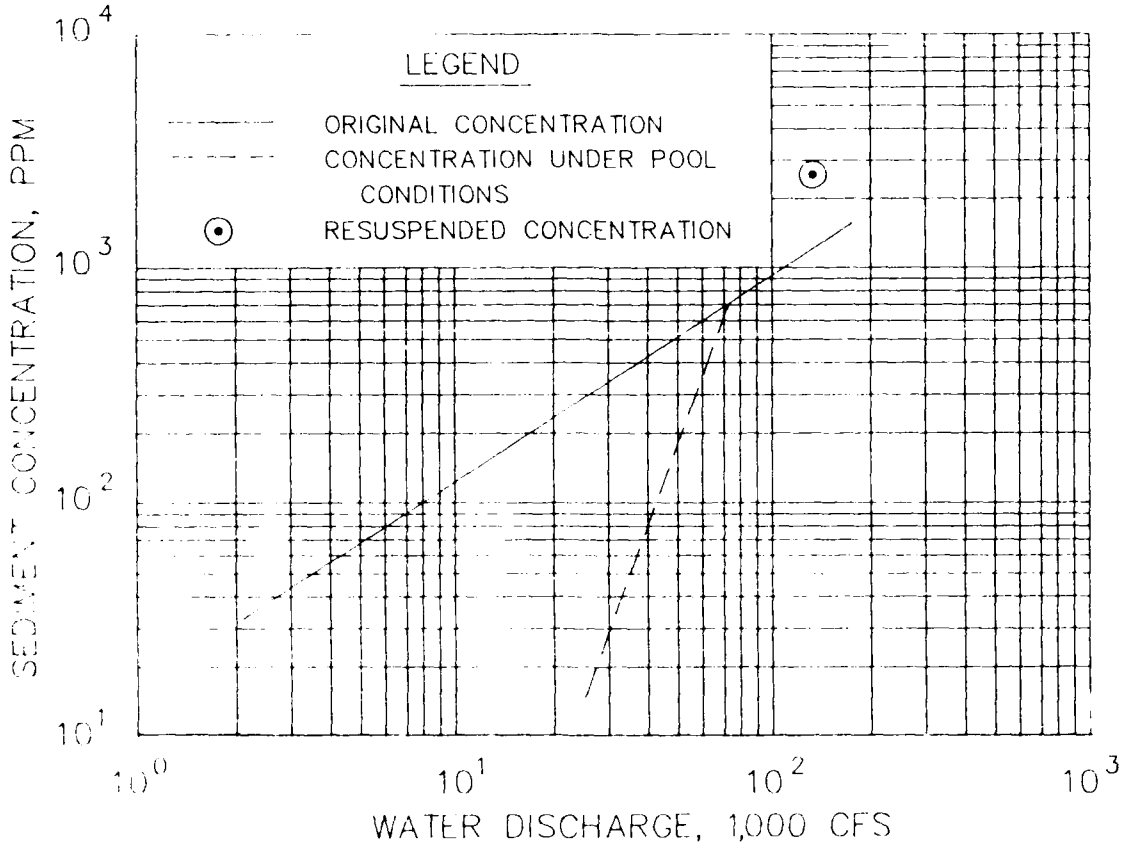

Figure 13. Sediment inflow rating curves for upstream reach

30. Deposition in the Lock and Dam No. 1 downstream lock approach channel measured between October 1984 and May 1985 was compared to calculated deposition using a sediment diffusion coefficient of 2 sq m/sec (Figure 14). This simulation was especially good for the first 500 ft downstream from the lock gate. For the next 1,000 ft, the model predicted about 75 percent of the measured deposition.

31. Deposition in the upstream lock approach channel at Lock and Dam No. 1 measured between 4 December 1985 and 17 December 1985 was compared to calculated deposition using sediment diffusion coefficients of 0.5, 2.0, and 25.0 sq m/sec. Figure 15 shows the area used for the comparison. The primary function of the sediment diffusion coefficients is to move fine sediments into the dead-water zones. The prototype measurements indicated that the material moved approximately 500 ft into the dead-water zone. Sediment diffusion coefficients of 0.5, 2.0, and 25.0 sq m/sec moved material 50, 600, and 1,200 ft respectively, into the dead-water zone.

32. The Lock and Dam No. 1 upstream and downstream numerical models

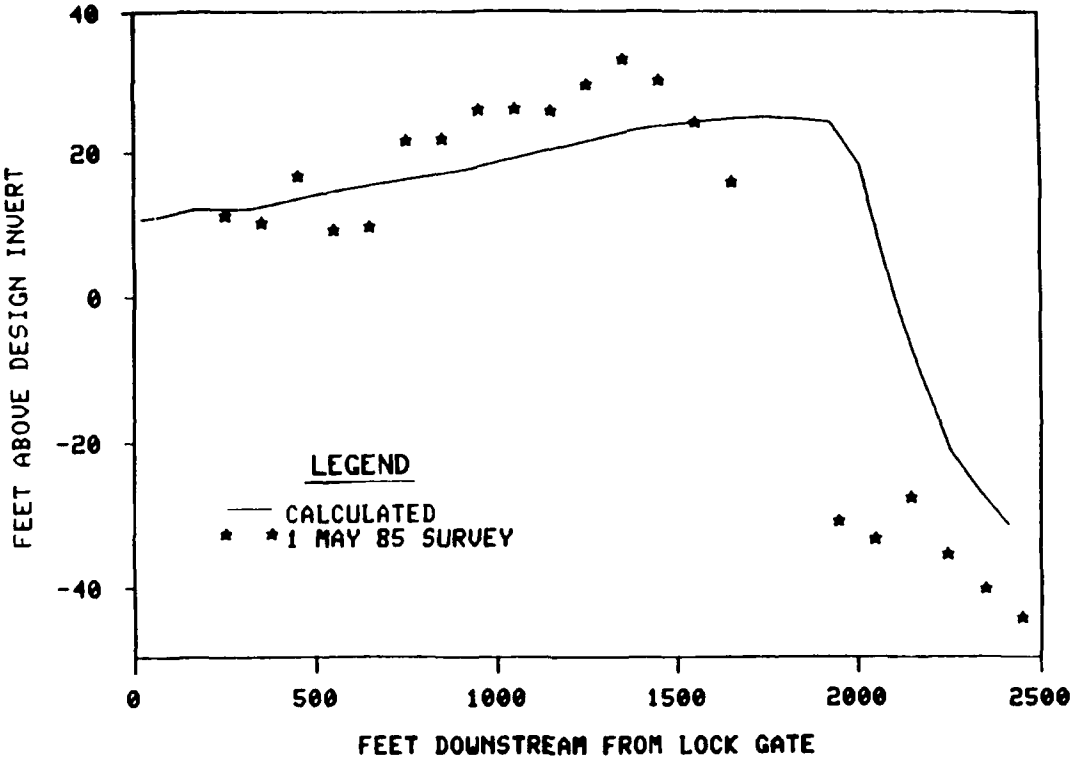

Figure 14. Comparison of measured and calculated deposition at Lock and Dam 1, downstream lock approach channel

were deemed to have successfully reproduced the prototype data in the primary area of interest using a sediment diffusion coefficient of 2.0 sq m/sec. This value was also used for the Lock and Dam No. 2 studies because hydraulic conditions and model grid resolution were similar.

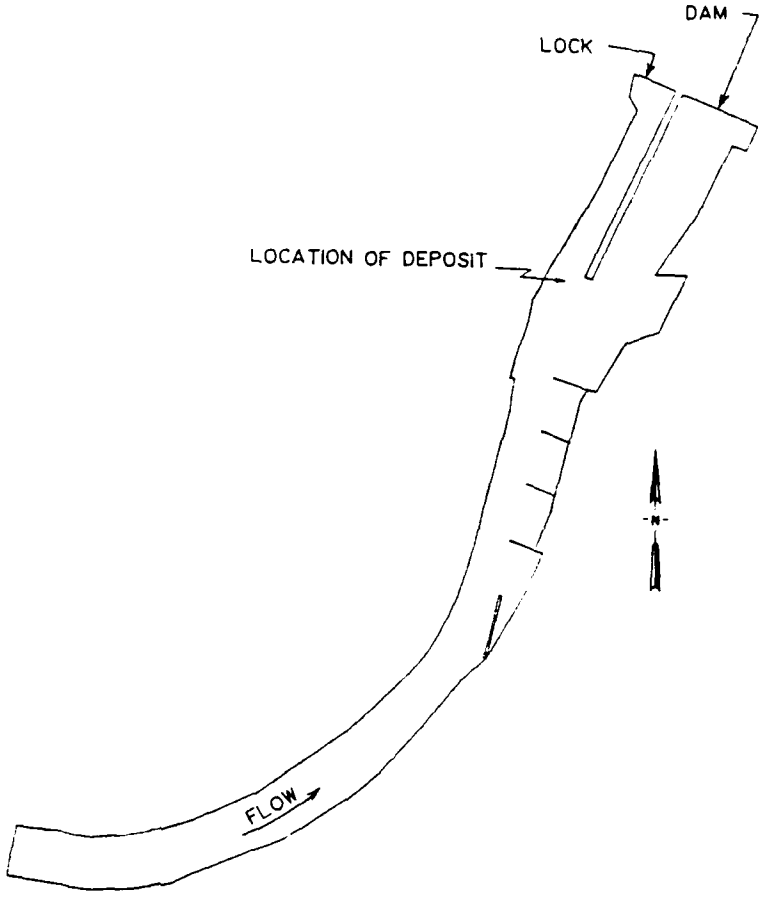

Figure 15. Deposit location upstream of Lock and Dam 1

PART III: MODEL RESULTS

Original Downstream Design

33. Velocity and sediment deposition patterns for 10-day simulations with steady-state discharges of 90,000 and 145,000 cfs were calculated for the original design, Plan C-81. Velocity patterns in the vicinity of the lock approach channel are shown in Plate 4. At both flow rates, a counterclockwise eddy developed in the lock approach channel. Eddy velocities were greatest just downstream from the unsubmerged portion of the longitudinal dike separating the lock approach and spillway exit channels. These hydrodynamic results were used to calculate sediment deposition in the lock approach channel. At a discharge Q of 90,000 cfs and a concentration C of 850 mg/ℓ, about 1.2 ft of material was deposited at the lock miter gate during the 10-day simulation, with the maximum deposition, about 2.5 ft, occurring about 800 ft downstream. At a discharge of 145,000 cfs and a concentration of 1,750 mg/ℓ, more than twice as much material was deposited, about 2.4 ft at the lock gate and 5.8 ft 800 ft downstream (Figure 16).

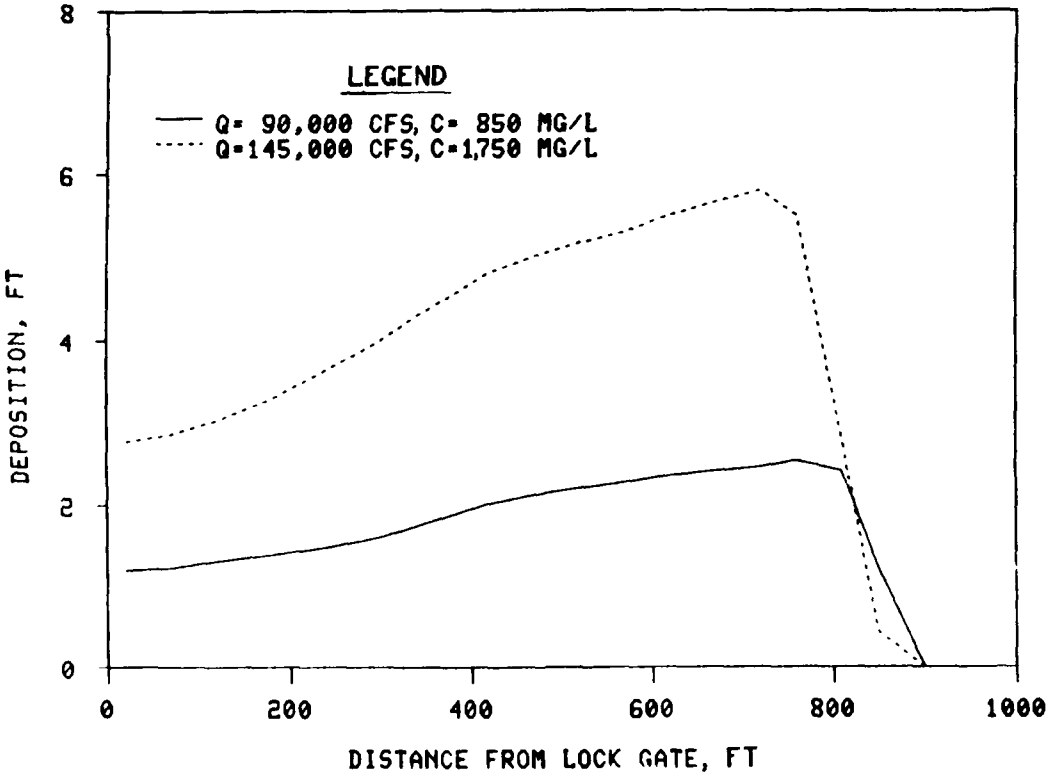

Figure 16. Deposition in downstream lock approach channel, 10-day hydrograph

34. These qualitative results were compared to calculated results at Lock and Dam No. 1 using similar boundary conditions: concentration 670 mg/ℓ, discharge 90,000 cfs, duration 10 days. The purpose of this exercise was to project the severity of deposition problems at Lock and Dam No. 2 based on the problems experienced at Lock and Dam No. 1 during the 1985 runoff event. Results of this comparison, shown in Figure 17, indicate that deposition at the downstream miter gate of Lock and Dam No. 2 will be about 45 percent that of Lock and Dam No. 1. The total volume of deposition in the lock approach channel will be much less at Lock and Dam No. 2 than at Lock and Dam No. 1.

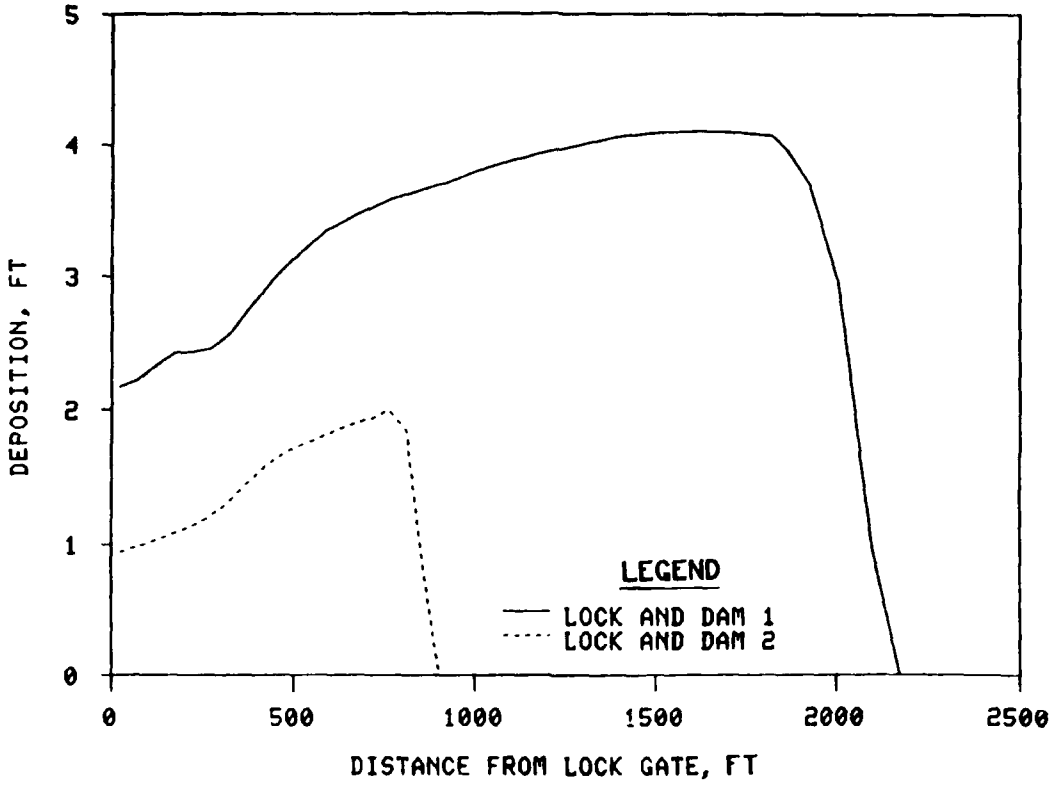

Figure 17. Deposition in downstream lock approach channel, 10-day simulation at 90,000 cfs, C = 670 mg/ℓ

35. The typical hydrograph was simulated using the numerical model to determine the average annual deposition. For this analysis, a modified regression curve based on historical data at Alexandria, LA, was used for the sediment inflow rating curve. About 8.1 ft of deposition was calculated at the lock miter gate with a maximum deposition of about 15.2 ft located 800 ft downstream (Figure 18). The vertical distance between the gate sill and the channel invert is 6.0 ft; therefore, some removal of deposited material will

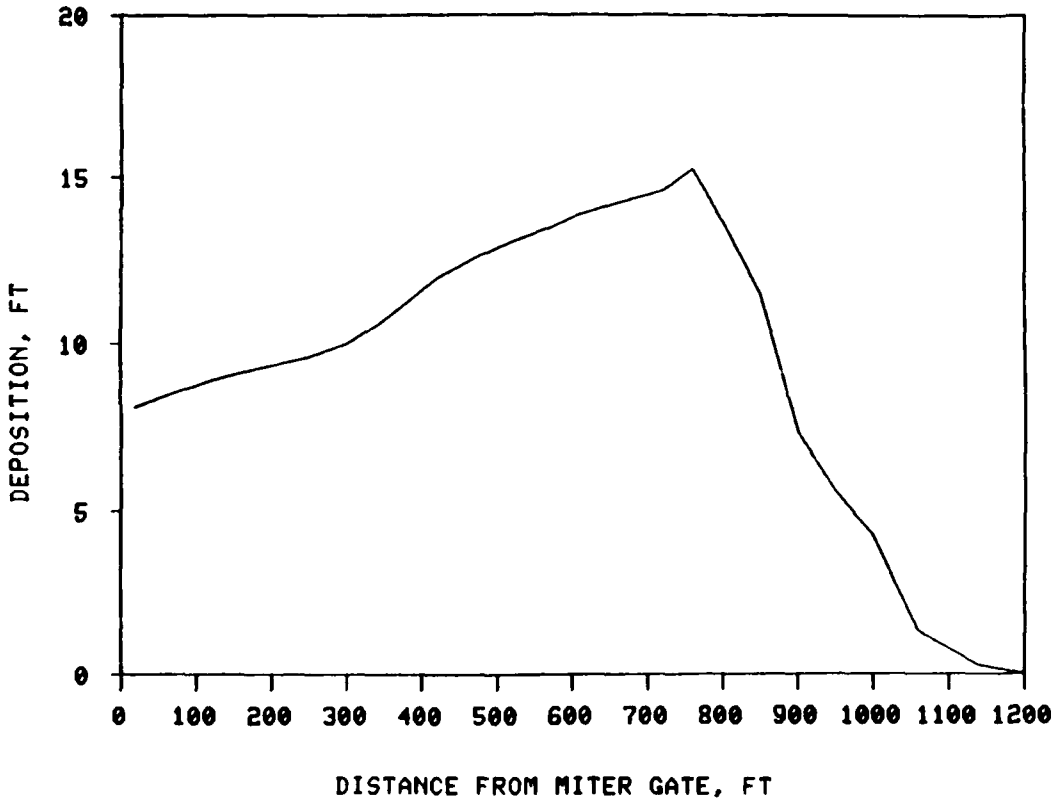

Figure 18. Deposition in downstream lock approach channel, typical hydrograph

be required on an annual basis. An average annual deposition of 70,000 cu yd was calculated.

Alternative Downstream Designs

36. The effect of varying the nature of the dikes dividing the lock approach and spillway exit channels was tested with the numerical model. Plans tested are shown in Figure 19.

37. In Plan C-137, all dikes, including the three dikes on the left descending bank, were removed leaving only the lock wing wall. In Plan C-138, the submerged dike was removed, leaving the lock wing wall and the exposed dike. With Plans C-137 and C-138, the right descending channel bank line was modified to account for shortening the barriers between the lock approach and main channels. In Plan C-139, the longitudinal submerged dike was raised above the water surface. Calculated velocity patterns for the original design and the three alternative plans are shown in Plates 5-8. Deposition in the lock approach channel for these plans is compared to the original plan, C-81,

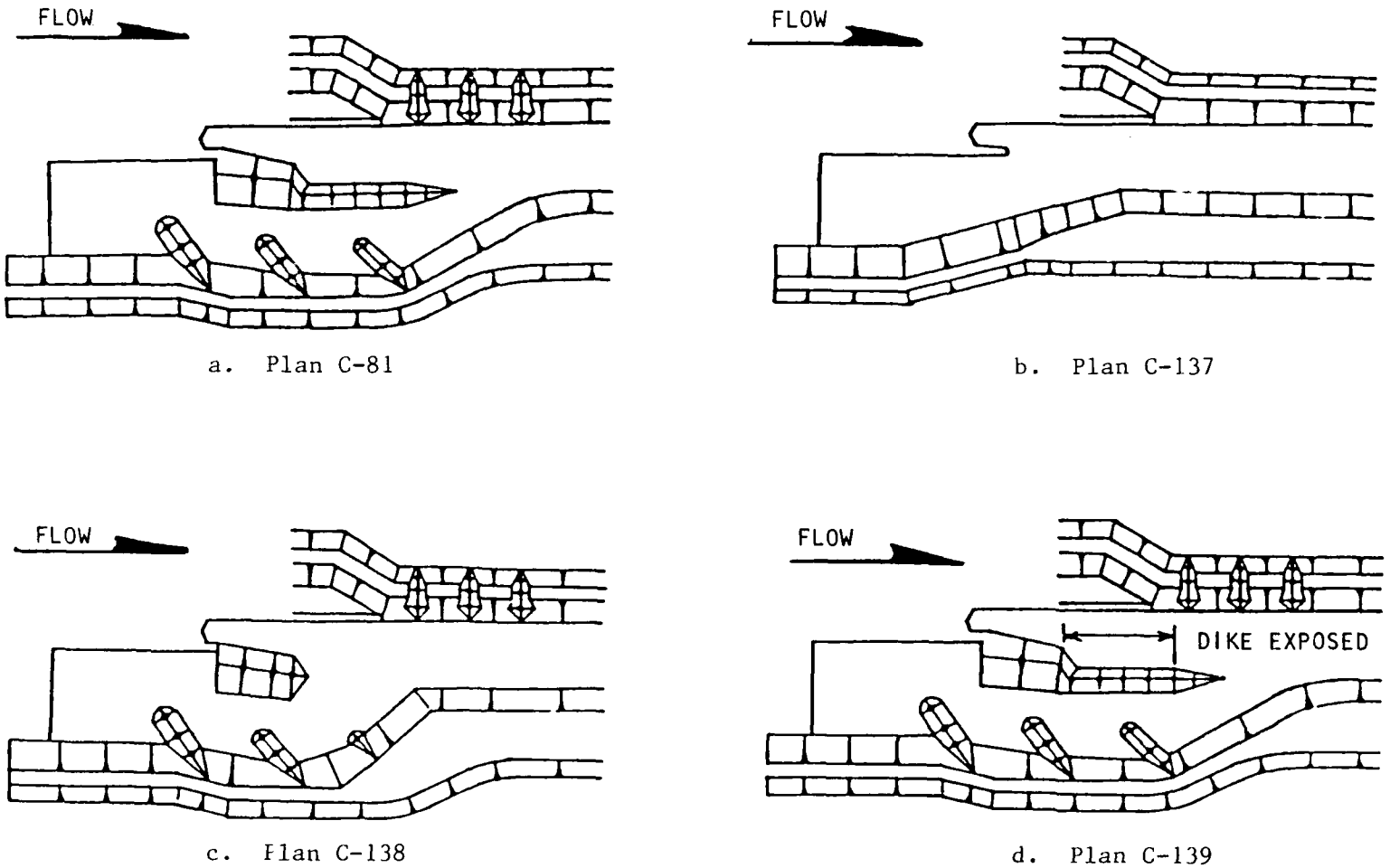

a. Plan C-81

b. Plan C-137

c. Plan C-138

d. Plan C-139

Figure 19. Alternate downstream plans

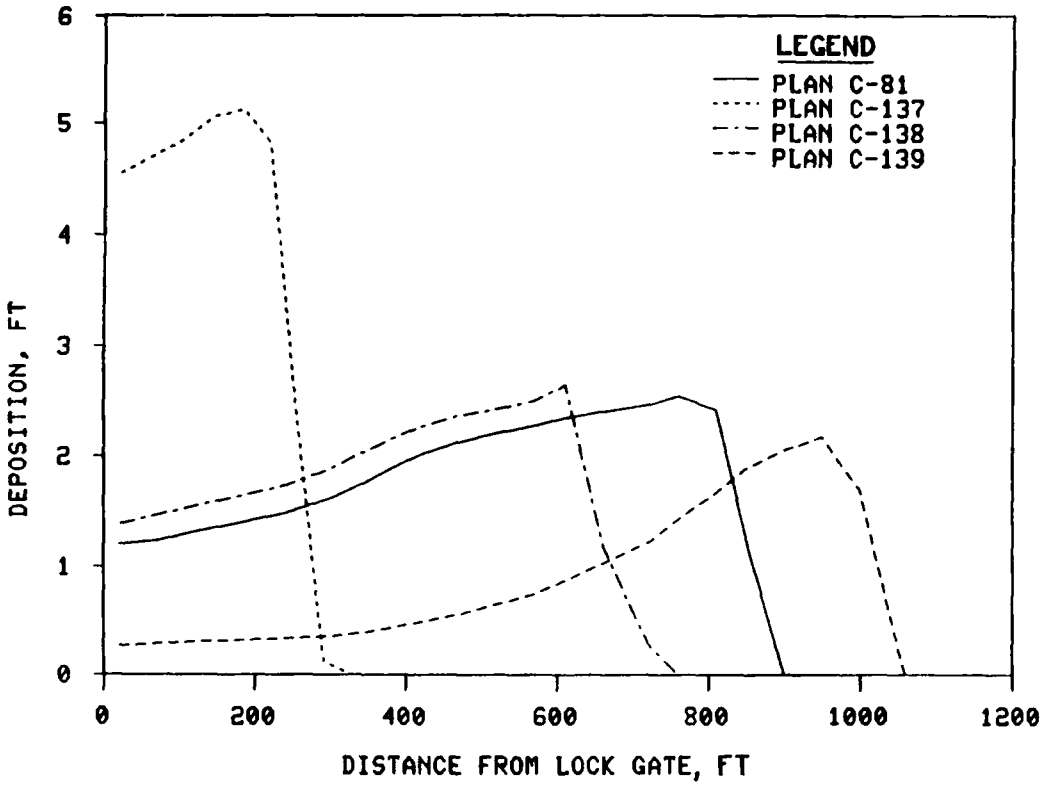

Figure 20. Deposition in downstream lock and approach channel, 10-day simulation at 90,000 cfs, C = 850 mg/ℓ

in Figure 20. Excessive deposition against the lock gate occurred with Plan C-137. A slight increase in deposition at the lock gate was offset by considerably less deposition downstream with Plan C-138. Plan C-139 resulted in the least amount of deposition at the lock gate. These results are consistent with results from the Lock and Dam No. 1 study, which showed that deposition at the lock gate is reduced as the confluence with flows from the main channel is moved away from the lock gate (Copeland and Thomas 1988). The suspended load deposition at the lock gate with the original design (Plan C-81) was about the same as was calculated at Lock and Dam No. 1 with a 400-ft extension of the I-wall. These results also indicate that the longitudinal submerged dike, which is effective in reducing bed-load deposition, does not reduce suspended load deposition in the lock approach channel.

Original Upstream Design

38. Velocity and sediment deposition patterns for 10-day simulations with steady-state discharges of 90,000 and 145,000 cfs were calculated for the

upstream original design. Two bottom geometries were considered, one representing the as-built conditions, the day the structure goes into operation, and the other representing some time in the future after the bed has adjusted to the new hydraulic conditions imposed by the dam. The latter geometry was obtained from the movable-bed physical model after simulating approximately 20 typical hydrographs. Plate 9 shows the bottom geometries for each condition. The hydrodynamic model indicated very little difference in the velocity patterns behind the guard wall for the two cases and the same general sediment depostion patterns occurred. Consequently, the as-built geometry was selected for additional testing. The sandbar located downstream of the three spur dikes (Plate 9, movable-bed geometry) was added to the as-built geometry to avoid the need to generate it with the numerical model. The sandbar was included because it formed very quickly in the physical model, and it influenced the velocity patterns in this area. Calculated velocity patterns for the two selected discharges are shown in Plate 10. For both flow rates, an outdraft began near the upstream end of the ported guard wall and continued downstream for the length of the wall. The model indicated that approximately 25 percent of the flow entered behind the guard wall. This agreed with measurements from the movable-bed physical model. Counterclockwise eddies developed near the right bank overflow weir and near the lock filling intake manifolds. These eddy locations proved to be areas of fine sediment deposition.

39. Plate 11 shows calculated sediment deposition that occurred over a 10-day period at each discharge. The plate shows only the reach of the model from the upstream confluence downstream to the dam. The sandbar on the right descending bank continued to grow and migrate downstream. The forecasted bottom geometry generated with the movable-bed physical model shown in Plate 9 indicates the extent to which this bar will grow. Some deposition occurred near the right descending overflow weir but should not cause a problem unless hydropower is installed. Deposition in the lock approach channel occurred on the left descending bank behind the guard wall and in the manifold area. The former should not cause a problem except possibly to the local boating ramp located near the downstream end of this area. The latter will inhibit operation of the miter gates. Figure 21 shows profiles on the lock center line of the deposit near the miter gates. Deposition at the miter gates was 3 and 9 ft at flows of 90,000 and 145,000 cfs, respectively. Both tests indicate

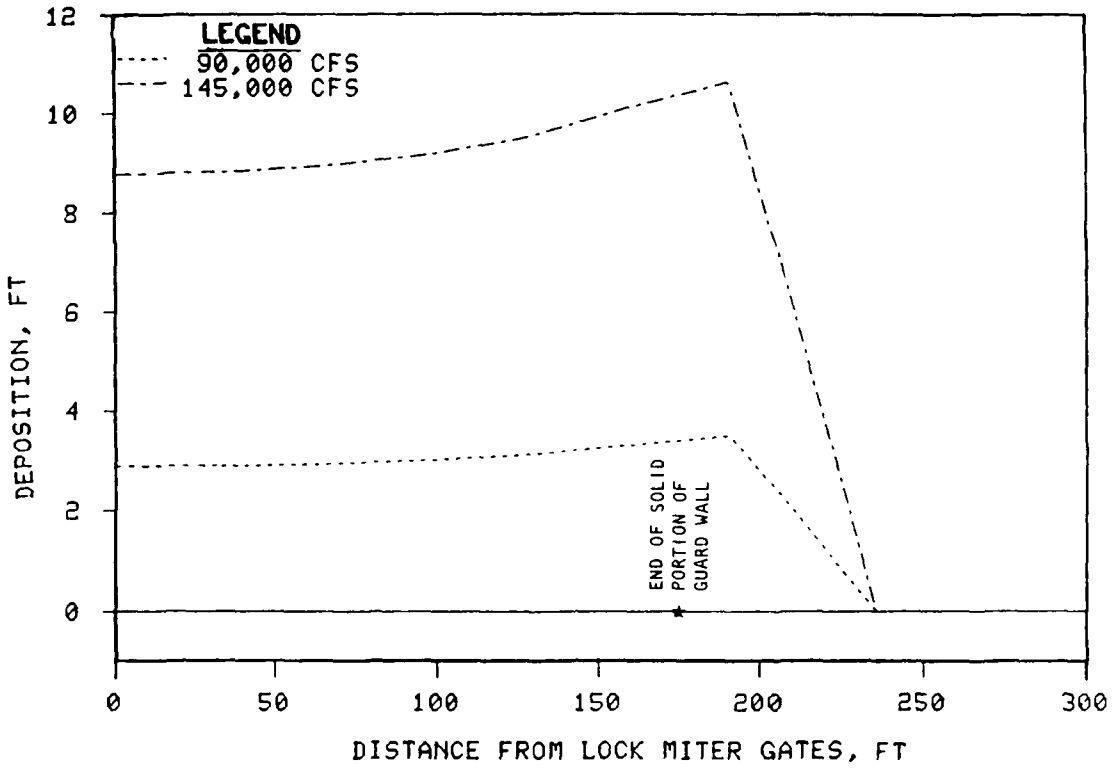

Figure 21. Deposition in upstream lock approach, as-built geometry, 10-day simulation

that the deposit will extend upstream to the most downstream port in the guard wall.

Alternative Upstream Designs

40. In an effort to prevent deposition at the miter gates, a solid guard wall was tested in the numerical model. The two discharges used for testing the original design were also tested in this plan. Plate 12 shows the velocity patterns for each. A pronounced outdraft occurred near the upstream end of the guard wall, and the eddy that was located near the miter gates in the original design moved upstream approximately 400 to 500 ft. Ten-day sedimentation tests were conducted at each discharge, and the resulting bed changes are shown in Plate 13. Deposits occurred in the same locations as with the ported guard wall, downstream of the sandbar and behind the solid guard wall. The 90,000-cfs discharge produced approximately 0.3 ft of deposition near the miter gates, and the 145,000-cfs discharge produced 1.2 ft. It appeared that the mechanism causing the deposit at the miter gates in the

original design was moved to the upstream end of the solid guard wall. This test indicates that the depth of the deposit near the miter gates is significantly reduced with a solid guard wall, even though the volume of the deposit is larger.

41. Several lengths of partially ported and partially solid guard walls were tested, always with the solid portion located at the downstream end. It was found that any reasonable portion of a ported wall on the upstream end of a solid wall allowed the sediment to flow behind the wall and be trapped by the solid wall. Results indicated that only the full-length solid guard wall reduced the deposition near the miter gates to an acceptable level.

42. As a result of navigation physical model studies at WES, it was concluded that the solid guard wall would cause too much outdraft. The Vicksburg District reported that the ported guard wall had already been constructed and would be difficult to modify. The wall was not structurally designed to be closed. Difficulty in dealing with these constraints resulted in a search for other solutions to the deposition problem at the miter gates.

43. Removal of the three dikes on the right descending bank was tested. It was reasoned that this modification would reduce the percentage of flow entering behind the ported guard wall, and hence less sediment would be transported into the area. The sandbar downstream of the dikes was also removed for these tests. Testing indicated that the crossing that occurs near the three dikes is a natural crossing and that the removal of the dikes would not reduce the flow rate behind the guard wall. The movable-bed physical model indicated that the presence of the three dikes was necessary to maintain minimum navagation depths. The three dikes were placed back into the numerical model.

44. Another method used to reduce the flow rate behind the ported guard wall was to construct a berm in the approach channel. Plate 14 shows the geometry of the approach channel with the berm in place. The berm, located on the left descending bank, began near the upstream end of the ported guard wall and extended upstream to the confluence with the old river channel. The maximum allowable berm elevation was determined to be 49.0 ft. The hydrodynamic model indicated that the berm reduced the volume of water flowing behind the ported guard wall by approximately 10 percent. However, the numerical sedimentation model indicated that the deposition near the miter gates was essentially the same as was calculated for the original design. A detailed

analysis of the flow field revealed that the flow distribution through the ported guard wall was shifted toward the downstream end of the wall when the berm was in place. This redistribution of flow along the guard wall was confirmed by tests conducted in the 1:50-scale physical model. As a result, the velocities driving the eddy near the miter gates were about the same for tests with and without the berm. When the velocities were the same and the system was able to carry the entire supply of very fine sands, the concentrations were the same; therefore, with or without a berm, the same amount of deposition occurred near the miter gates.

45. The berm was also tested in the navigation and movable-bed physical models. None of the three models indicated any adverse effects due to the berm. The berm was incorporated into the design to reduce excavation costs.

46. A representative portion of the typical annual hydrograph was simulated. In an effort to avoid excessive computer costs, the five discharges between 15 December 1971 and 20 January 1972 from the typical hydrograph were simulated (Plate 3). Analyses of the remaining discharges and their respective concentrations indicated that they would not significantly contribute to the deposition problem near the miter gates. The concentration curve used in these tests considered the effect of the pool on the suspended load. The methods used to generate the curve are discussed in paragraphs 26-28. Sedimentation results of this partial hydrograph test indicate that about 12 ft of material deposited at the miter gates and extended upstream to the most downstream port in the ported guard wall (Figure 22). The volume of deposit was less than 10,000 cu yd, but the resulting bed elevation will inhibit miter gate operations.

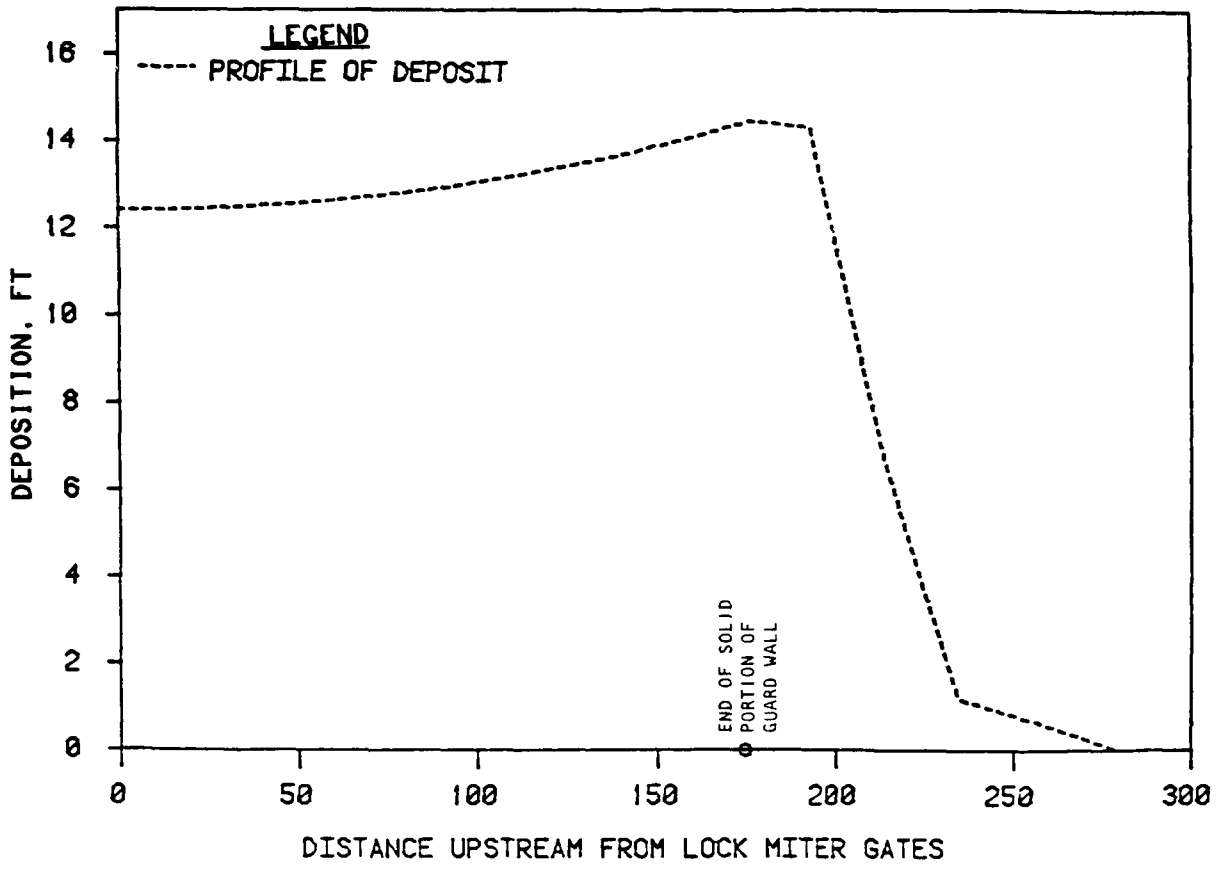

Figure 22. Deposits near upstream miter gates, typical hydrograph

PART IV: CONCLUSIONS AND RECOMMENDATIONS

47. The two-dimensional numerical model study demonstrated that there will be significant suspended sediment deposition problems in front of the miter gates at Lock and Dam No. 2 with the proposed design.

48. Deposition at the miter gate in the downstream lock approach channel is projected to be about 8 ft during a typical year. With a distance of 6.7 ft between the gate sill and the channel invert, some dredging or other mechanical removal technique will be necessary during the annual runoff event to ensure opening and closing of the miter gates. Deposition problems will be more severe during high-flow years. Average annual dredging in the downstream lock approach channel will be about 70,000 cu yd. Conditions could be improved by raising the longitudinal submerged dike, thus moving the confluence of the lock approach and spillway channels downstream.

49. Deposition of fine sediment near the upstream miter gates at Lock and Dam No. 2 will be significant. The ported guard wall brings large quantities of sediment-laden flow close to the lock gates. Using a typical hydrograph, the model predicted 12 ft of deposition at the miter gates annually. In order to maintain miter gate operations, removal of the material will be necessary after the deposit forms to approximately 6 ft deep. Although the ported guard wall creates maintenance problems, it was determined by navigation physical model studies to be necessary. Study results indicate that sediment deposition at the lock gates would be essentially eliminated by constructing a solid guard wall.

50. This study has demonstrated that with the adopted design at Lock and Dam No. 2, sedimentation problems will occur at the lock gates on an annual basis. Mechanical removal contingencies will need to be provided.

REFERENCES

Ackers, P., and White, W. R. 1973 (Nov). "Sediment Transport: New Approach and Analysis," Journal, Hydraulics Division, American Society of Civil Engineers, Vol 99, No. HY11, Paper No. 10167, pp 2041-2060.

Copeland, Ronald R., and Thomas, William A. 1988 (Jun). "Red River Waterway Sedimentation Study, Downstream from Lock and Dam No. 1; Numerical Model Investigation," Technical Report HL-88-15, US Army Engineer Waterways Experiment Station, Vicksburg, MS.

Limerinos, J. T. 1970. "Determination of the Manning Coefficient from Measured Bed Roughness in Natural Channels," Water-Supply Paper 1989-B, US Geological Survey, Reston, VA.

Little, C. D., Jr. 1985. "Use of a Two Dimensional Modeling System to Evaluate Lock Channel Shoaling on Lock and Dam No. 1 on the Red River Waterway," Proceedings of 15th Mississippi Water Resources Conference, 27-28 February 1985, Jackson, MS, Mississippi Water Resources Research Institute, Mississippi State University, Starkville, MS.

Maynord, S. T., and Markussen, J. V. "Red River Waterway, John H. Overton Lock and Dam, Stilling Basin, Riprap, and Hydropower Requirements; Spillway and Hydropower Hydraulic Model Study" (in preparation), Report No. 4, US Army Engineer Waterways Experiment Station, Vicksburg, MS.

O'Neal, C. W. "Red River Waterway, John H. Overton Lock and Dam, Sedimentation Conditions; Hydraulic Model Investigation" (in preparation), Report 3, US Army Engineer Waterways Experiment Station, Vicksburg, MS.

Thomas, William A., and McAnally, William H., Jr. 1985 (Jul). "User's Manual for the Generalized Computer Program System: Open-Channel Flow and Sedimentation, TABS-2," Instruction Report HL-85-1, US Army Engineer Waterways Experiment Station, Vicksburg, MS.

US Army Engineer District, New Orleans. 1980a (Feb). "Red River Waterway, Louisiana, Texas, Arkansas, and Oklahoma - Mississippi River to Shreveport, Louisiana," Hydrology, Design Memorandum No. 3 (Revised), New Orleans, LA.

_____. 1980b (Feb). "Red River Waterway, Louisiana, Texas, Arkansas, and Oklahoma - Mississippi River to Shreveport, Louisiana," Design Memorandum No. 18, New Orleans, LA.

Wooley, R. T. "Red River Waterway, John H. Overton Lock and Dam, Navigation Alignment Conditions; Hydraulic Model Investigation" (in preparation), Report 2, US Army Engineer Waterways Experiment Station, Vicksburg, MS.

Table 1

Effect of Submerged Dike Adjustments on Velocity

Location*	Physical Model Velocity fps	Numerical Model Velocity, fps			
		n = 0.06 E = 200	n = 0.06 E = 500	n = 0.20 E = 25	n = 0.06 E = 25
1	3.9	3.9	3.9	4.1	3.9
2	4.7	4.8	4.8	5.1	4.8
3	6.0	5.6	5.5	5.9	5.6
4	6.9	6.4	6.5	5.8	6.2
5	7.8	7.5	7.5	5.9	7.7
6		4.1	4.4	5.5	4.0
7	7.1	6.7	6.7	7.8	6.8
8	7.5	6.4	6.4	7.2	6.5
9	7.1	6.0	5.9	5.1	6.0
10	7.0	5.4	5.3	3.7	5.5
11	7.4	7.1	7.0	8.4	7.2
12	8.1	7.2	7.1	8.2	7.3
13	8.9	7.5	7.5	7.2	7.6
14	8.7	8.5	8.4	5.7	8.4
15		5.3	5.5	6.3	5.2
16	7.8	6.5	6.3	4.0	6.9
17	6.3	6.4	6.0	7.5	7.3
18	8.2	7.5	7.5	8.7	7.6
19	9.2	7.7	7.5	6.5	7.6
20	7.9	8.8	7.1	5.7	8.8
21	5.1	3.9	4.3	5.4	3.5
22		1.1	1.3	2.6	0.9
23	1.6	3.2	3.3	2.9	2.9
24	3.6	4.2	4.2	2.9	4.0
25	4.9	5.2	5.1	2.8	5.2
26	5.1	5.8	5.6	3.4	6.1
27	7.4	6.6	6.4	7.3	7.0
28	8.6	6.6	6.5	8.0	6.8
29	8.6	6.5	6.3	6.9	6.6
30	6.8	6.2	6.2	5.3	6.2
31		5.8	6.0	5.0	5.7
32	5.1	5.4	5.7	5.4	5.1
33	4.8	4.6	4.7	5.8	4.3
34	2.6	3.1	3.2	3.2	2.8
35	4.6	4.2	4.2	3.4	4.0
36	4.3	5.2	5.1	3.7	5.2
37	4.6	5.8	5.7	4.4	6.1

(Continued)

Note: n = Manning's roughness coefficient, E = turbulent exchange coefficient. A blank indicates that no measurement was taken in the physical model.

* Shown in Plate 1.

Table 1 (Concluded)

Location	Physical Model Velocity fps	Numerical Model Velocity, fps			
		n = 0.06 E = 200	n = 0.06 E = 500	n = 0.20 E = 25	n = 0.06 E = 25
38	7.7	6.5	6.4	7.0	6.9
39	8.7	6.8	6.7	7.9	7.0
40	7.4	6.8	6.7	7.2	6.9
41		6.6	6.6	6.3	6.6
42	5.6	6.2	6.2	6.0	6.1
43		5.8	5.8	6.1	5.5
44		5.5	5.5	6.1	5.2
45	5.9	4.6	4.6	5.6	4.4

Table 2

Effect of Turbulent Exchange Coefficients on Velocity

Location*	Physical Model Velocity fps			Numerical Model Velocity, fps				
	1	2	3	E = 5	E = 10	E = 25	E = 50	E = 500
1	5.5		3.9	4.4	4.0	3.9	4.0	4.1
2	6.5		4.7	5.0	4.9	4.8	4.8	4.6
3	7.1		6.0	5.6	5.6	5.6	5.6	5.2
4	7.7		6.9	6.3	6.2	6.2	6.2	5.6
5	6.4		7.8	8.1	7.9	7.8	7.6	6.8
6	4.9			4.2	4.2	4.0	3.8	4.6
7	7.0		7.1	6.8	6.7	6.8	6.9	5.8
8	8.1		7.5	6.3	6.3	6.4	6.5	6.0
9	7.3		7.1	5.9	5.9	6.1	6.0	5.8
10	7.2		7.0	5.6	5.6	5.6	5.5	5.5
11	7.9		7.4	7.2	7.2	7.3	7.0	5.7
12	8.0		8.1	7.1	7.1	7.3	7.3	6.3
13	9.5		8.9	7.5	7.5	7.5	7.5	7.0
14	9.4		8.7	8.5	8.6	8.6	8.6	8.3
15				5.6	5.5	5.2	5.0	6.1
16	7.2		7.8	7.4	7.3	7.1	6.9	5.0
17	7.1		6.3	7.4	7.4	7.2	7.0	5.1
18	8.9		8.2	7.4	7.5	7.4	7.3	6.0
19	9.3		9.2	7.5	7.6	7.6	7.6	6.7
20	7.9		7.9	9.1	9.0	8.7	8.9	8.4
21			5.1	3.6	3.4	3.5	3.5	4.9
22		-1.6		-0.8	-0.4	0.7	1.2	2.0
23		0.0	1.6	2.4	2.7	2.9	2.9	3.1
24	5.7	4.6	3.6	4.3	4.3	4.1	3.9	3.6
25	6.7	5.5	4.9	6.0	5.8	5.4	5.1	4.2
26	5.5	5.1	5.1	6.5	6.5	6.3	5.9	4.8
27	6.2	6.6	7.4	7.1	7.1	6.9	6.6	5.3
28	7.5	8.4	8.6	6.8	6.8	6.8	6.6	5.6
29	8.0	8.3	8.6	6.7	6.7	6.7	6.5	5.9
30	7.2	6.7	6.8	6.6	6.5	6.3	6.1	6.0
31		4.8		6.1	6.0	5.8	5.6	6.0
32	5.6	4.8	5.1	5.4	5.3	5.2	5.1	6.0
33		4.6	4.8	4.7	4.6	4.5	4.5	5.8
34		2.5	2.6	2.5	2.7	2.8	3.1	3.1
35	5.5	4.2	4.6	4.6	4.4	4.1	4.0	4.0
36	6.5	4.6	4.3	5.8	5.6	5.4	5.2	4.8
37	6.3	4.8	4.6	6.5	6.3	6.1	5.9	5.3
38	6.6	7.6	7.7	7.0	6.9	6.8	6.5	5.8
39	8.4	7.9	8.7	7.1	7.0	7.0	6.8	6.3

(Continued)

Note: A blank indicates that no measurement was taken in the physical model.
* Shown in Plate 2.

Table 2 (Concluded)

Location	Physical Model Velocity fps			Numerical Model Velocity, fps				
	1	2	3	E = 5	E = 10	E = 25	E = 50	E = 500
40	6.7	6.8	7.4	7.1	7.0	6.9	6.8	6.5
41				6.8	6.8	6.6	6.5	6.6
42	5.8	5.1	5.6	6.5	6.4	6.2	6.2	6.7
43				5.8	5.8	5.7	5.6	6.4
44				5.5	5.4	5.4	5.4	6.3
45		6.0	5.9	4.8	4.7	4.6	4.6	5.9

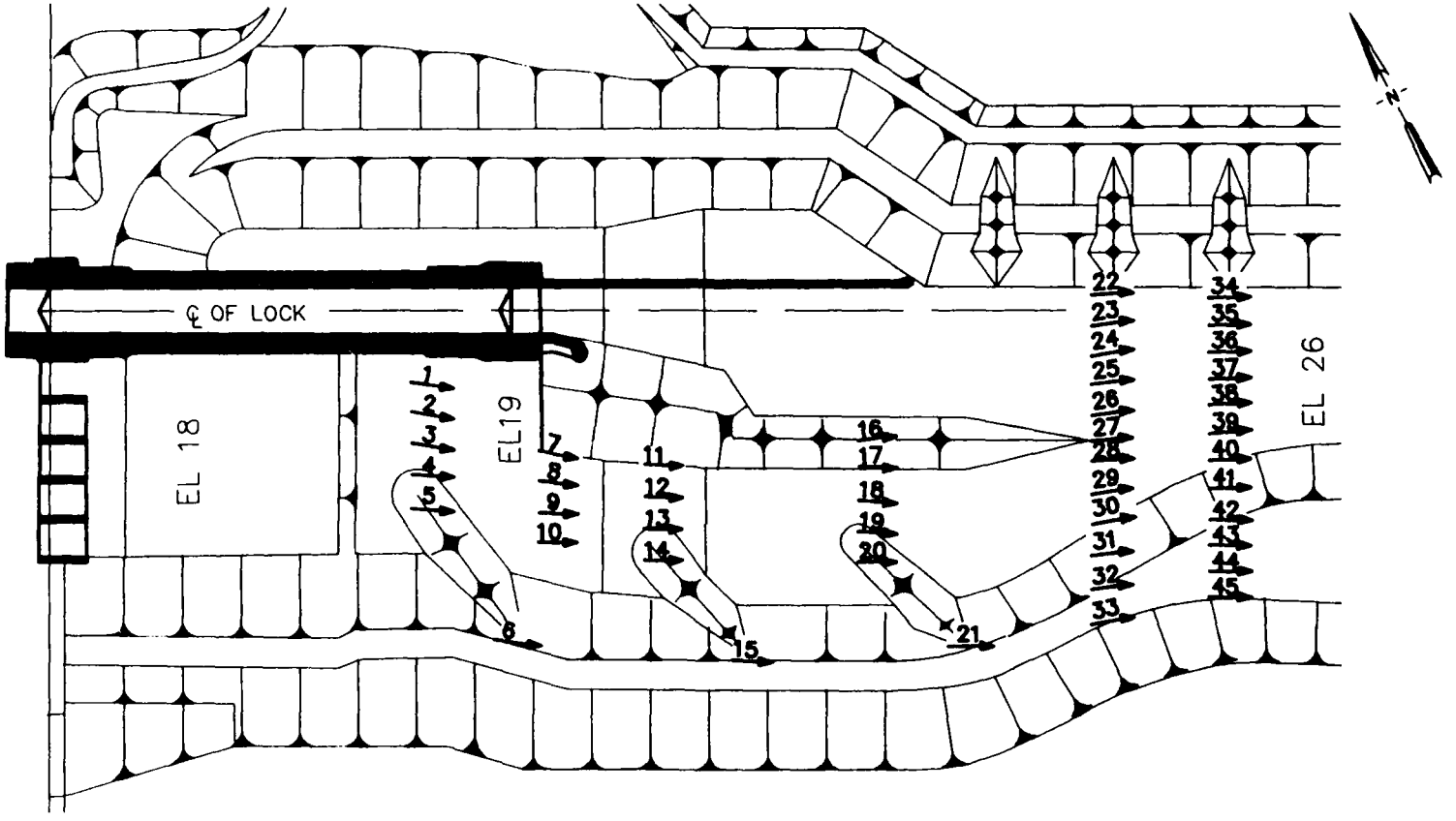

NOTE: LOCATIONS CORRESPOND TO THOSE RECORDED IN TABLES 1 AND 2.

LOCATION OF MEASURED AND CALCULATED VELOCITIES

PLAN C-81

PLATE 1

PLATE 2

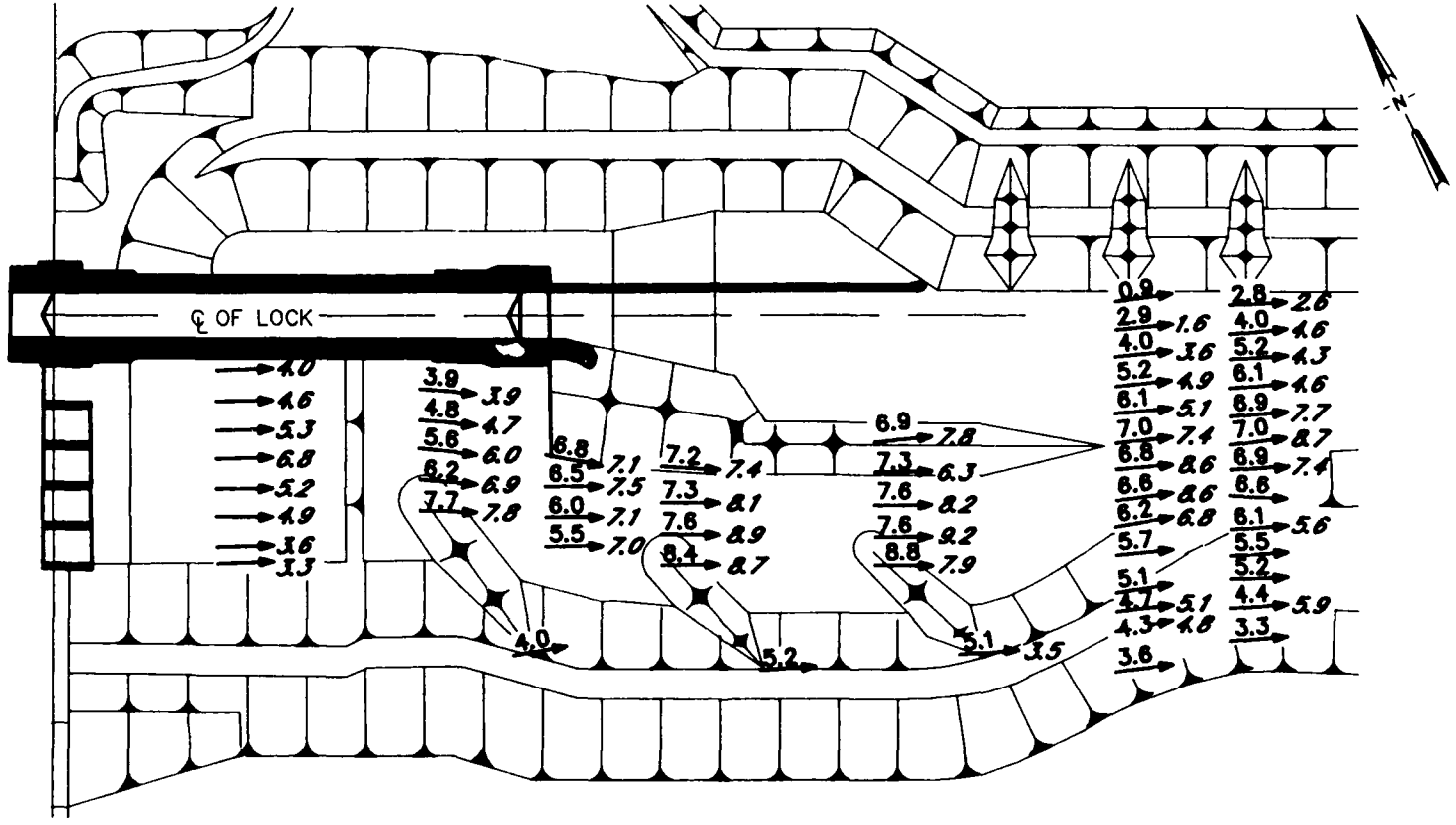

NOTES: VELOCITIES MEASURED IN PHYSICAL MODEL AT 60 PERCENT OF DEPTH BELOW WATER SURFACE.

CALCULATED VELOCITIES IN FEET PER SECOND ARE LOCATED OVER VELOCITY VECTORS.

MEASURED VELOCITIES IN FEET PER SECOND ARE LOCATED AT END OF VELOCITY VECTORS.

MEASURED AND CALCULATED VELOCITIES

PLAN C-81

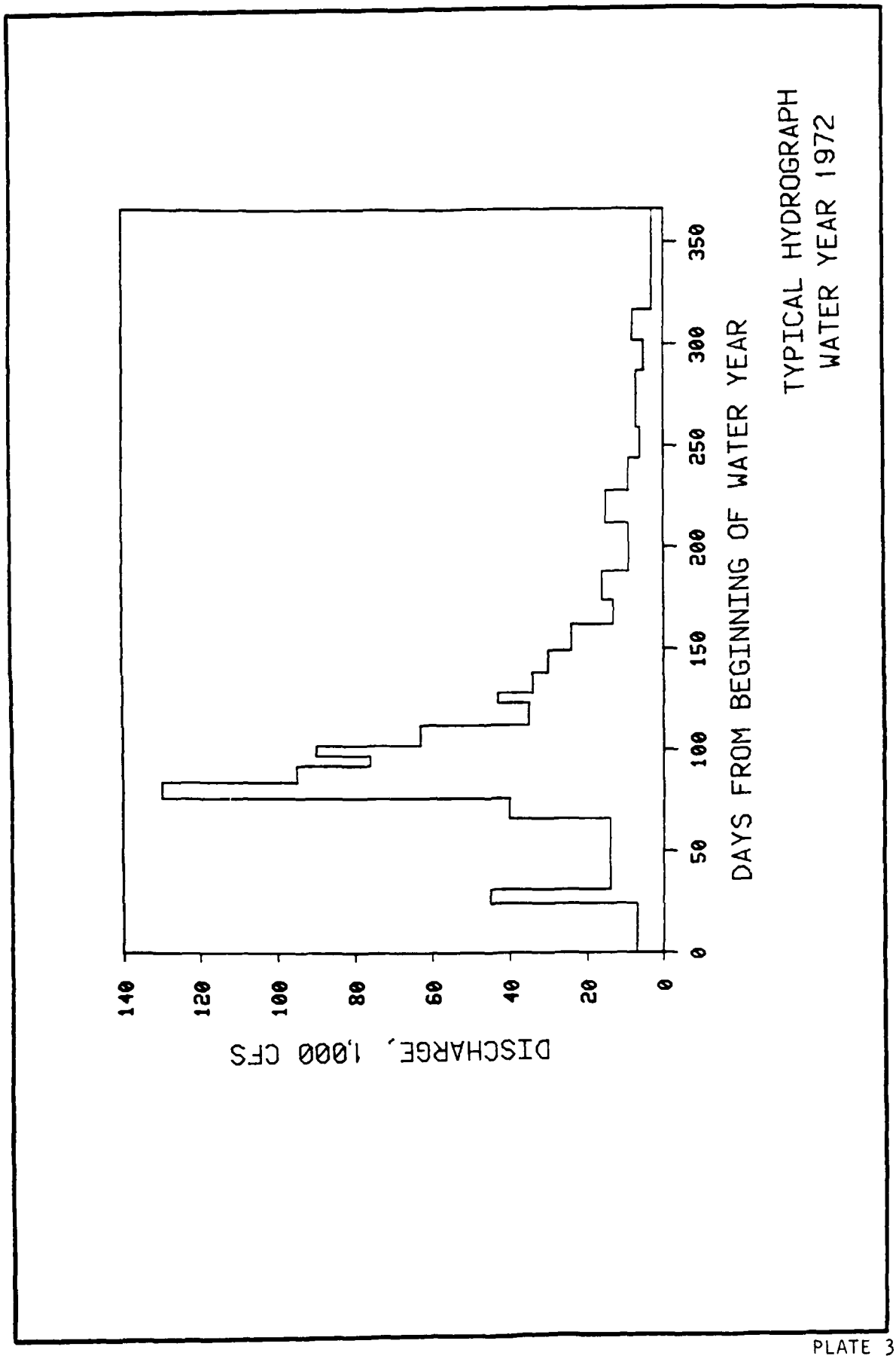
TYPICAL HYDROGRAPH
WATER YEAR 1972
DAYS FROM BEGINNING OF WATER YEAR
0
50
100
150
200
250
300
350
DISCHARGE, 1,000 CFS
0
20
40
60
80
100
120
140

PLATE 3

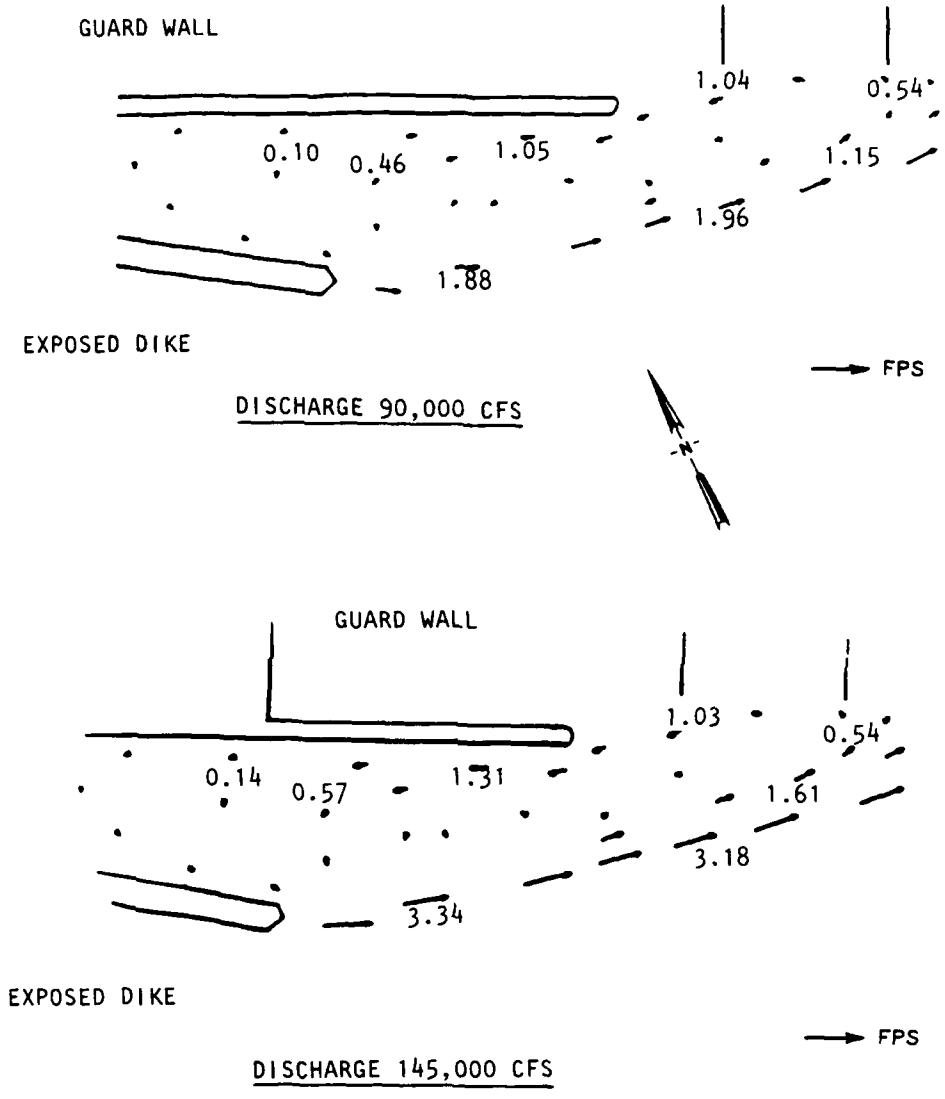

VELOCITY PATTERNS
VICINITY OF LOCK APPROACH CHANNEL
ORIGINAL DESIGN (PLAN C-81)

PLATE 4

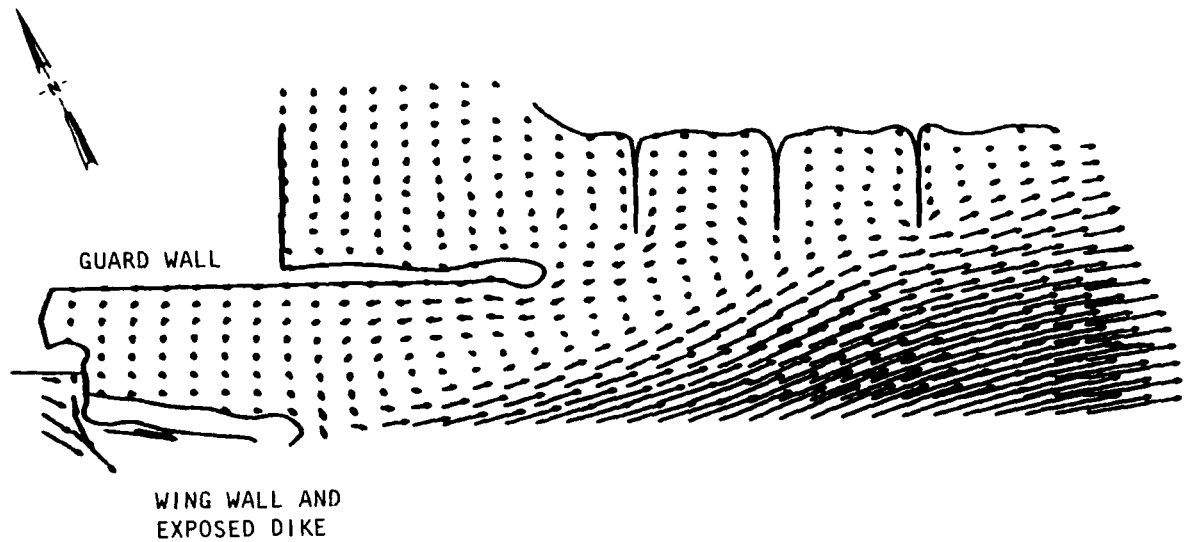

VELOCITY PATTERNS
DOWNSTREAM LOCK APPROACH CHANNEL
PLAN C-8I
DISCHARGE 90,000 CFS

PLATE 5

PLATE 6

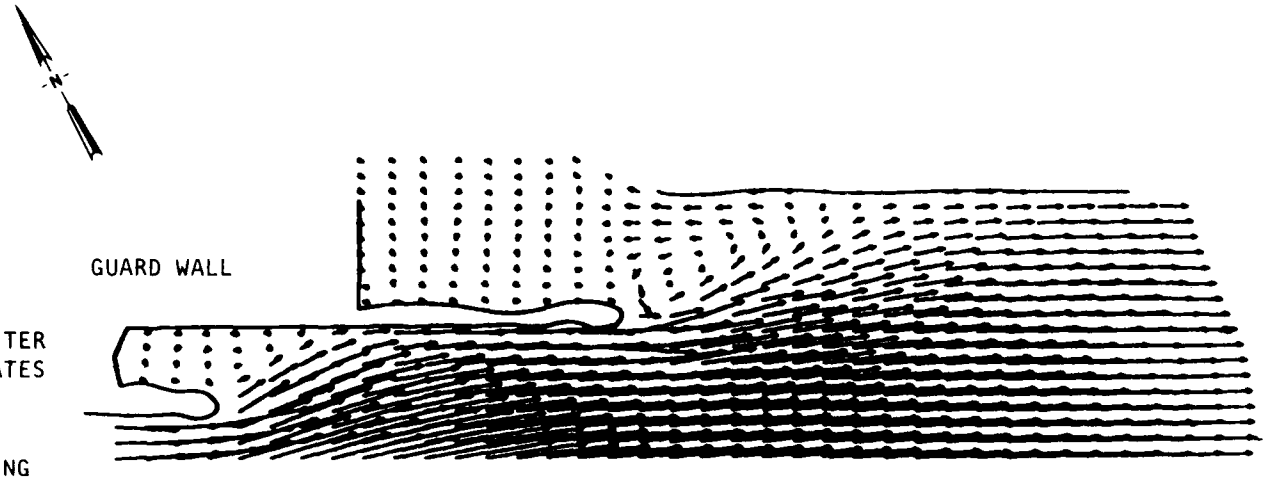

VELOCITY VECTOR SCALE

4.0 FPS

4.0

VELOCITY PATTERNS
DOWNSTREAM LOCK APPROACH CHANNEL
PLAN C-137
DISCHARGE 90,000 CFS

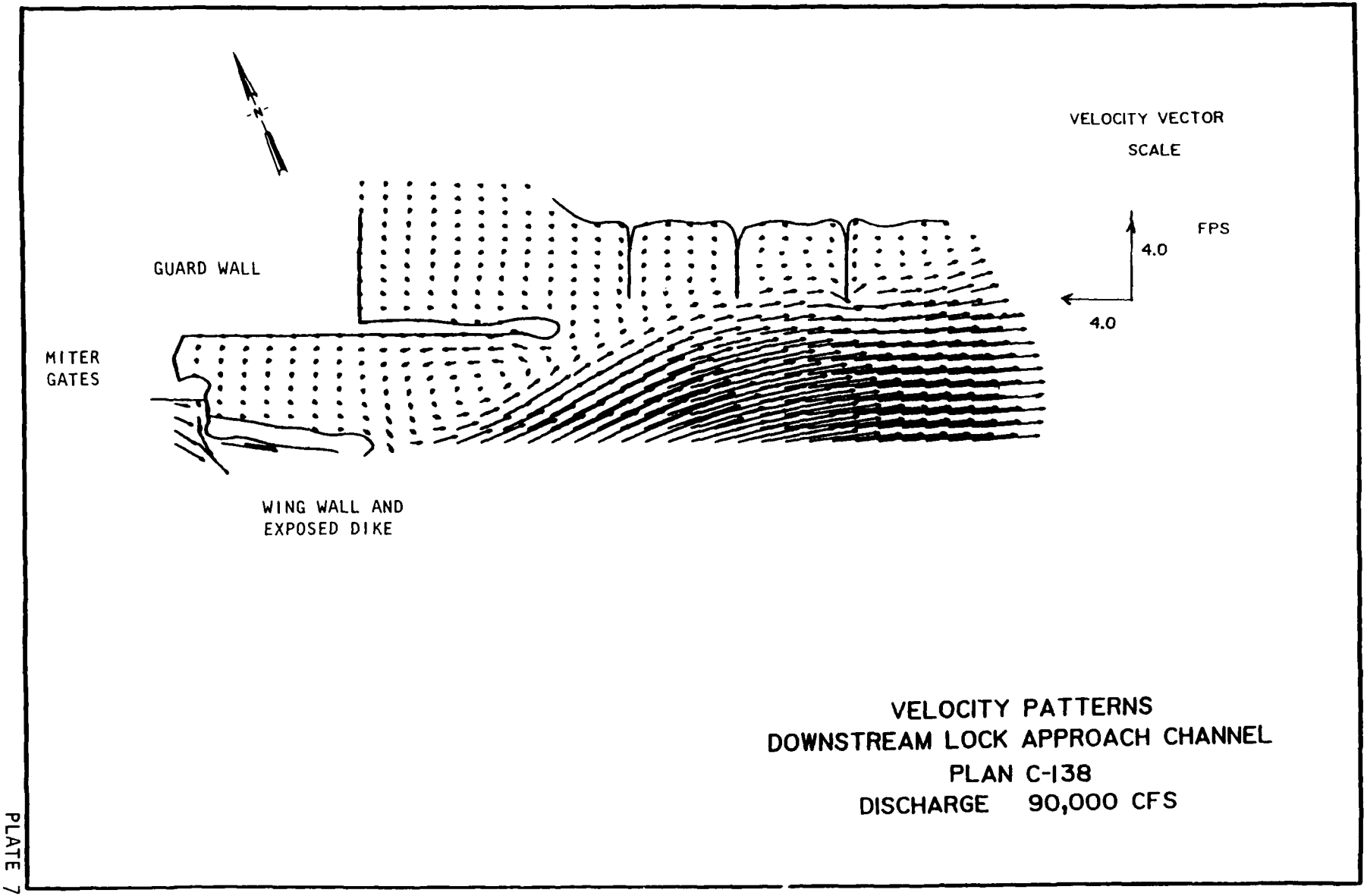

VELOCITY PATTERNS
DOWNSTREAM LOCK APPROACH CHANNEL
PLAN C-138
DISCHARGE 90,000 CFS

PLATE 7

PLATE 8

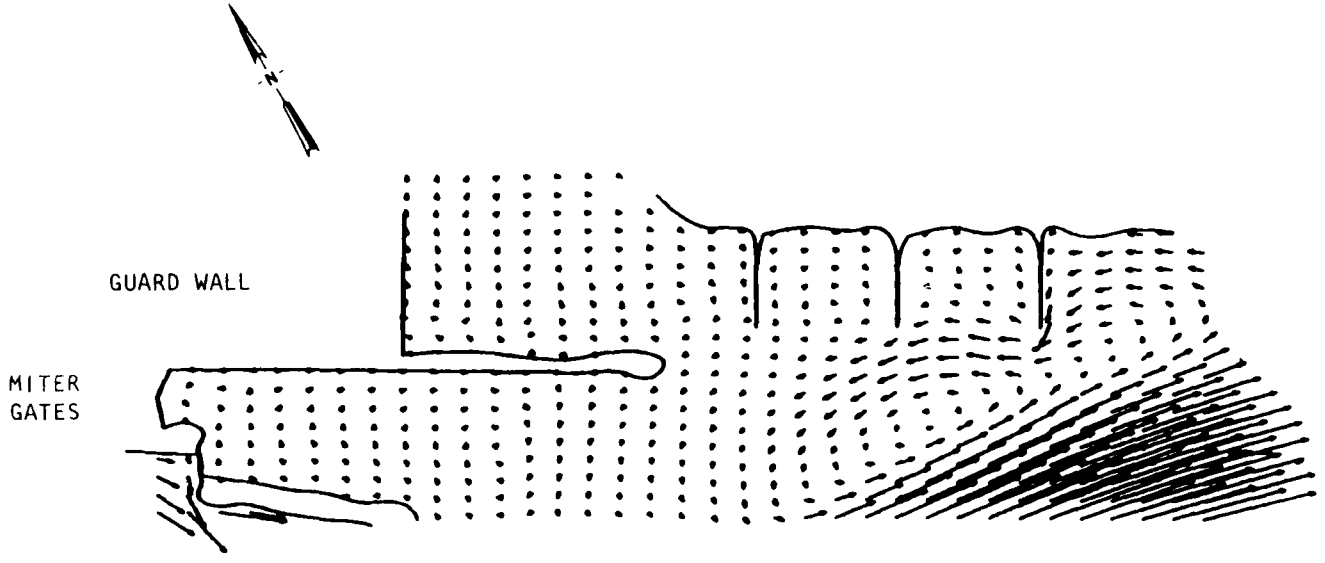

VELOCITY VECTOR SCALE

FPS
4.0
4.0

VELOCITY PATTERNS
DOWNSTREAM LOCK APPROACH CHANNEL
PLAN C-139
DISCHARGE 90,000 CFS

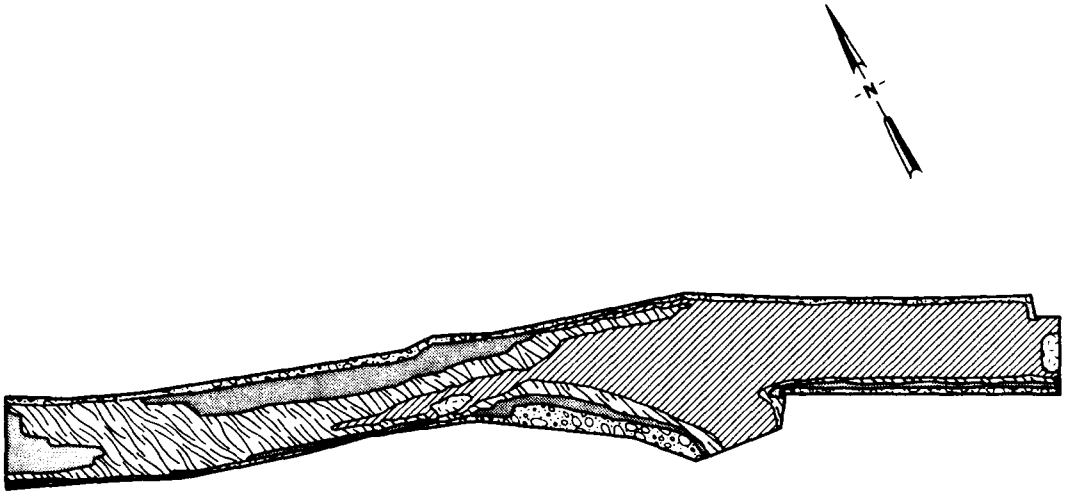

AS-BUILT GEOMETRY

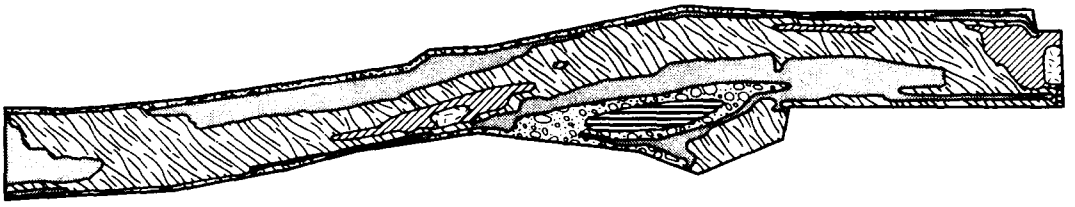

MOVABLE-BED GEOMETRY

BED ELEVATION, FT

15.1 - 25	45.1 - 55
25.1 - 35	55.1 - 65
35.1 - 45	65.1 - 75

UPSTREAM BED GEOMETRY

PLATE 9

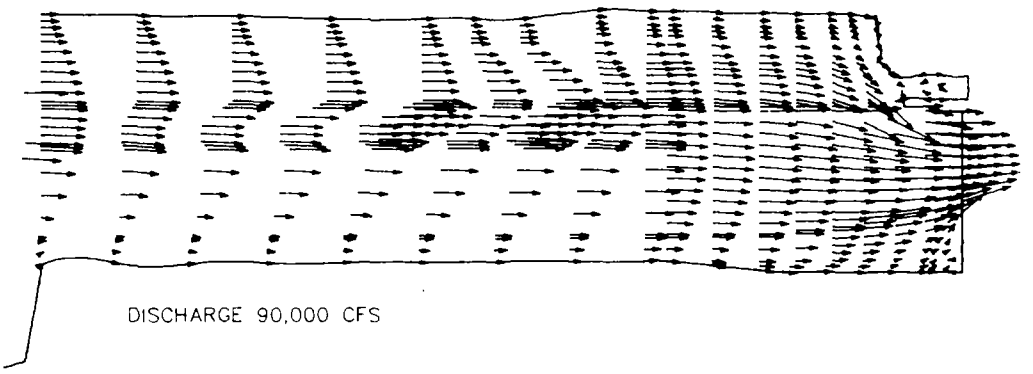

DISCHARGE 90,000 CFS

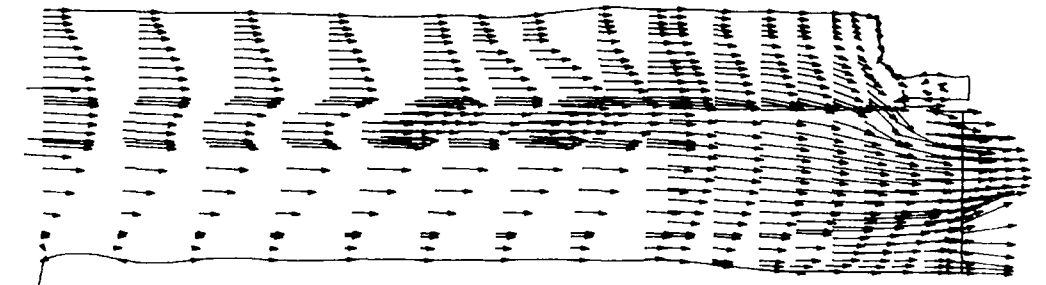

DISCHARGE 145,000 CFS

VELOCITY VECTOR SCALE
(FPS)

CALCULATED VELOCITY PATTERNS
IN UPSTREAM LOCK APPROACH CHANNEL
AS-BUILT GEOMETRY

PLATE 10

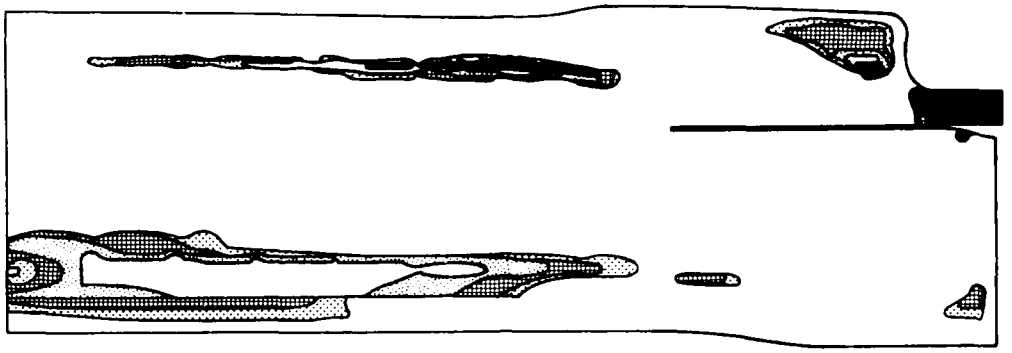

DISCHARGE 90,000 CFS

SEDIMENT DEPOSITION, FT

0.00 - 1.00	2.01 - 2.50
1.01 - 1.50	2.51 - 3.00
1.51 - 2.00	3.01 - 3.50

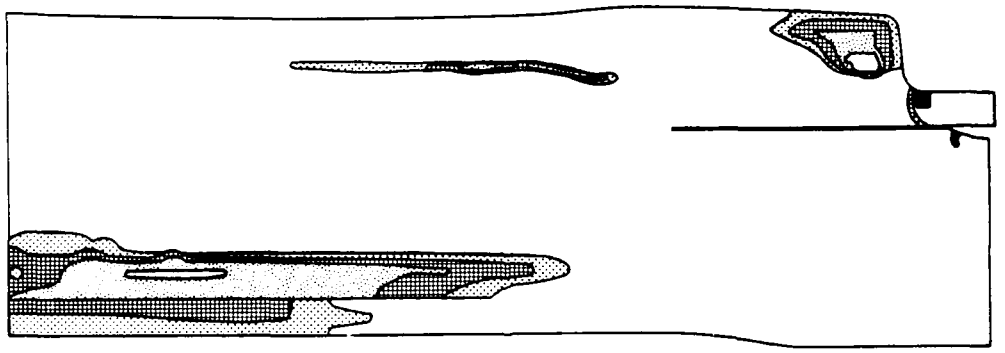

DISCHARGE 145,000 CFS

SEDIMENT DEPOSITION, FT

0.00 - 2.00	6.01 - 8.00
2.01 - 4.00	8.01 - 10.00
4.01 - 6.00	10.01 - 12.00

AS-BUILT GEOMETRY, PORTED GUARD WALL
SEDIMENT DEPOSITION, 10 DAYS ELAPSED TIME

PLATE 11

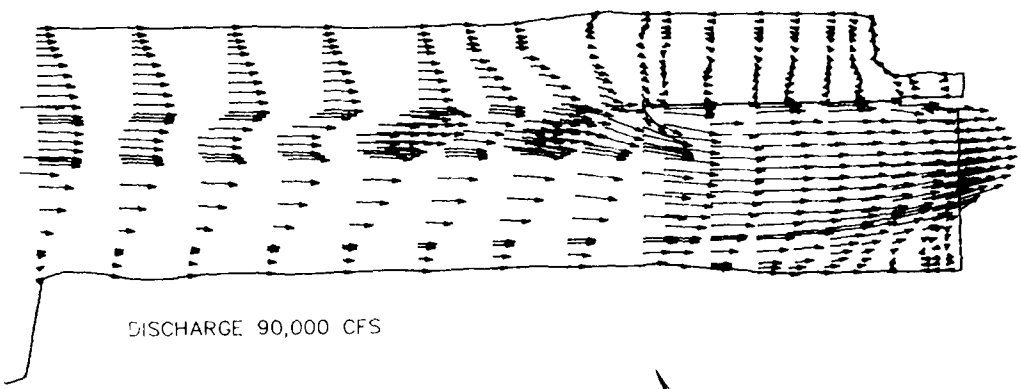

DISCHARGE 90,000 CFS

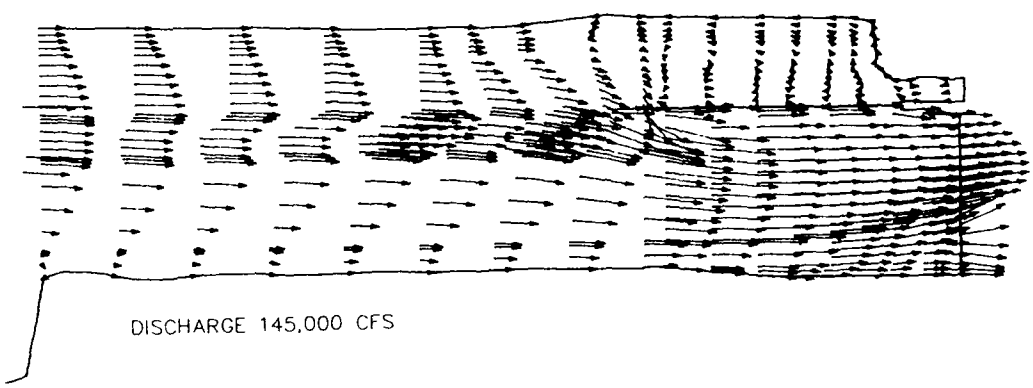

DISCHARGE 145,000 CFS

VELOCITY VECTOR SCALE
(FPS)

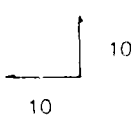

CALCULATED VELOCITY PATTERNS
IN UPSTREAM LOCK APPROACH CHANNEL
SOLID GUARD WALL

PLATE 12

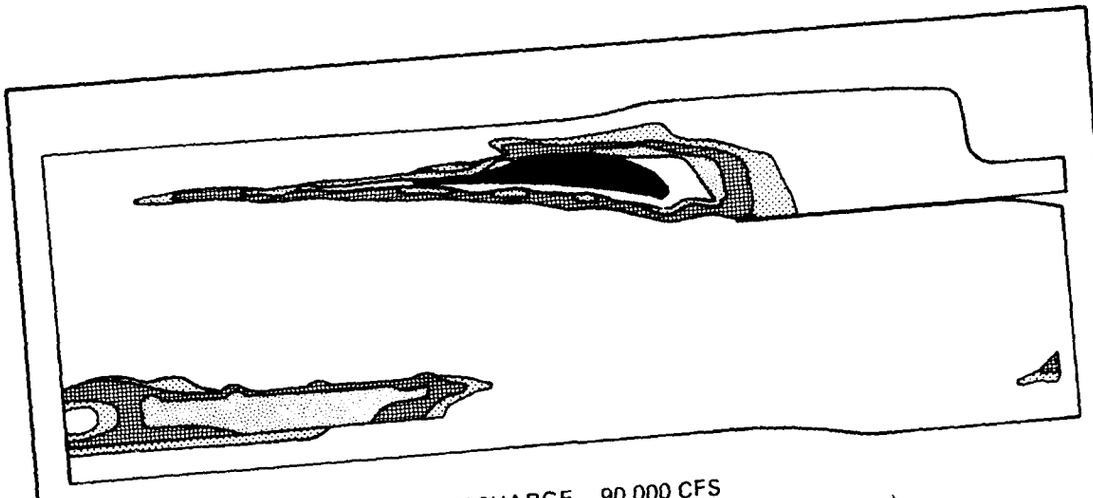

DISCHARGE 90,000 CFS

SEDIMENT DEPOSITION, FT

0.00 - 1.50	2.51 - 3.00
1.51 - 2.00	3.01 - 3.50
2.01 - 2.50	3.51 - 4.00

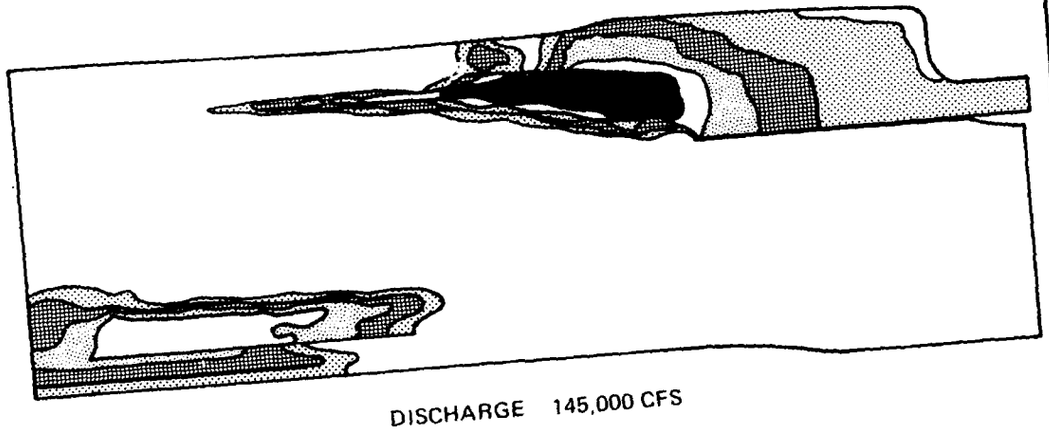

DISCHARGE 145,000 CFS

SEDIMENT DEPOSITION, FT

0.00 - 1.00	5.01 - 7.00
1.01 - 3.00	7.01 - 9.00
3.01 - 5.00	9.01 - 11.00

AS-BUILT GEOMETRY, SOLID GUARD WALL
SEDIMENT DEPOSITION, 10 DAYS ELAPSED TIME

PLATE 13

PLATE 14

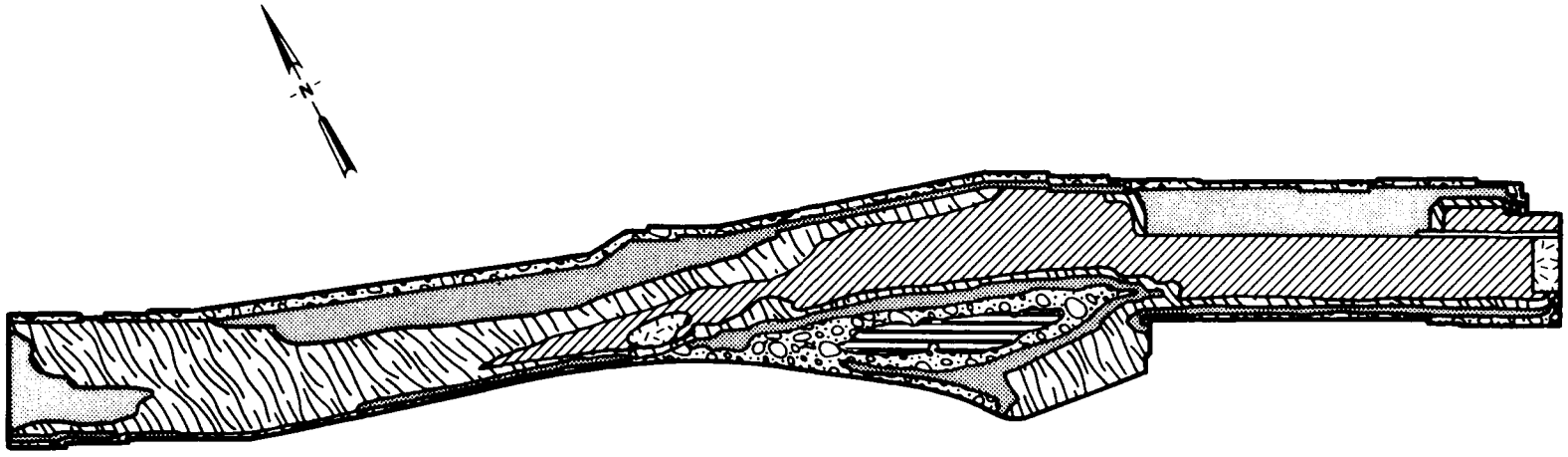

AS BUILT-GEOMETRY WITH BERM EL 49.0

BED ELEVATION, FT

15.1 - 25.0	45.1 - 55.0
25.1 - 35.0	55.1 - 65.0
35.1 - 45.0	65.1 - 75.0

LOCK AND DAM NO. 2
ALTERNATIVE UPSTREAM BED GEOMETRY